A Cell Decomposition Approach to Robotic Trajectory Planning via Disjunctive Programming

by

Ashleigh Swingler

Department of Mechanical Engineering and Materials Science
Duke University

Date: _____

Approved:

_____
Silvia Ferrari, Supervisor

_____
Ronald Parr

_____
Xiaobai Sun

Thesis submitted in partial fulfillment of the requirements for the degree of Master of Science in the Department of Mechanical Engineering and Materials Science in the Graduate School of Duke University
2012

Abstract

A Cell Decomposition Approach to Robotic Trajectory Planning via Disjunctive Programming

by

Ashleigh Swingler

Department of Mechanical Engineering and Materials Science
Duke University

Date: _____

Approved:

_____
Silvia Ferrari, Supervisor

_____
Ronald Parr

_____
Xiaobai Sun

An abstract of a thesis submitted in partial fulfillment of the requirements for the degree of Master of Science in the Department of Mechanical Engineering and Materials Science in the Graduate School of Duke University
2012

Abstract

This thesis develops a novel solution method for the problem of collision-free, optimal control of a robotic vehicle in an obstacle populated environment. The technique presented combines the well established approximate cell decomposition methodology with disjunctive programming in order to address both geometric and kinematic trajectory concerns. In this work, an algorithm for determining the shortest distance, collision-free path of a robot with unicycle kinematics is developed. In addition, the research defines a technique to discretize nonholonomic vehicle kinematics into a set of mixed integer linear constraints. Results obtained using the Tomlab/CPLEX mixed integer quadratic programming software exhibit that the method developed provides a powerful initial step in reconciling geometric path planning methods with optimal control techniques.

For Shaka and Skabenga,

the best research assistants a graduate student could have.

Contents

List of Figures

List of Abbreviations and Symbols

Symbols

$\mathcal{W}$	Workspace
$\mathcal{A}$	Robot geometry
$\mathcal{B}$	Stationary workspace obstacle
$\mathcal{F}_{\mathcal{A}}$	Moving Cartesian reference frame embedded in $\mathcal{A}$
$\mathcal{F}_{\mathcal{W}}$	Stationary workspace reference frame
Θ	Rotation range
$\mathcal{C}$	Configuration space
$\mathcal{CB}$	C-Obstacle
$\mathcal{C}_{free}$	Obstacle free configuration space
$\mathcal{K}_{void}$	Set of void ACD cells
$\mathbf{x}$	State variables of the robot
$\mathbf{u}$	Control variables of the robot
κ	Void cell of the ACD
M	Large positive number
T	Finite horizon time
N	Number of discrete time steps
Δt	Length of a discrete time step
δ	Decision variables corresponding to the system dynamics
ϕ	Discretized rotation angle

$\mathcal{G}$	Cell connectivity graph
η	Entry node
$\mathcal{G}^{\eta}$	Entry node connectivity
$\mathcal{T}$	Connectivity Tree
b	Branch
β	Decision variables corresponding to the tree branches
J	Optimization function

1

Introduction

Robotic path planning algorithms have, in recent years, garnered significant attention in the controls and intelligent systems community. This surge in research is due to the growing need for autonomous systems in both military and civilian arenas. The development of optimal trajectory planners has been motivated by scenarios such as land-mine detection, reconnaissance and surveillance, search and rescue missions, monitoring of endangered species, multi-agent network connectivity, and optimization of manufacturing plant procedures. These applications give rise to motion planning problems subject to various constraints. The constraints range from obstacle avoidance to kinematic and dynamic considerations. Numerous algorithms have been developed to provide solutions for the multitude of motion planning problems.

This research will consider the benchmark problem of a single robot navigating between defined initial and final configurations in an obstacle populated environment, in which the positions and the geometries of the stationary obstacles are assumed known *a priori*. In order to understand the various classes of solution methods motion planning problem, some common concepts are reviewed first. The *workspace* refers to the actual physical space containing the obstacles and traversed by the vehicle,

[1]. The number of parameters required to define the configuration of the system is referred to as the *degrees of freedom* (DOF) of the system. The *configuration space* is the space containing all possible configurations of the robot; the dimension of the configuration space is equal to the DOF of the vehicle.

Planning techniques are categorized based on a variety of aspects. A method is defined as *global* if it takes into account the entire workspace of the problem during all stages of motion planing. By contrast, *local* planners only address the area of the workspace in the immediate vicinity of the vehicle. Motion planning methodologies are further categorized as *complete* or *incomplete*. A complete planner guarantees a solution in environments where a solution is feasible, [1]. A method is incomplete if it does not guarantee the return of a solution. These algorithms are further categorized as potential field approaches, roadmap and kinodynamic methods, cell decompositions, or mathematical programming techniques.

In *potential field* methods the vehicle is considered to be a particle under the influence of an artificial workspace potential function, [2]. Obstacles are modeled as repulsive potentials, while the goal configuration is an attractive potential, [3]. Once the potential function over the workspace has been determined, the algorithm follows the negative gradient of the potential function toward the goal position (or a local minimum). Potential field approaches are effective path planning methods for a number of problems, including point-like vehicles with nonholonomic constraints on the state variables, [4, 5]. To address the computational requirements of implementing many potential field methods, randomized sampling techniques have been developed to lessen these requirements. Although numerically more efficient, randomized algorithms do not offer the path repeatability of other techniques, as two runs of the same motion planning problem may return different paths, [3]. These planners are also unable to efficiently determine failure in environments where no feasible paths exist, [3]. In addition, potential field methods are only applicable to

vehicles with limited DOFs, [5]. Furthermore, this class of algorithms is particularly sensitive to local minima, [6, 7]. As a result, focus in this field has been on developing techniques to avoid issues with local minima. A number of approaches has recently been developed to address this historically limiting aspect of potential field methods. However, these new techniques are not without weaknesses. A drawback of the potential field class of problems is that in large workspaces, with many concave obstacles, determining an expression for the potential becomes cumbersome to compute, [1]. Another major disadvantage of potential field methods is that the solutions found are likely only locally optimal, [6]. Furthermore, controllers for nonholonomic vehicles may not be easy to design within the framework of potential field methods, particularly for robots with higher DOF.

The second class is referred to as *roadmap*, or skeleton, methods. These techniques preprocess the obstacle-free space of the workspace into a roadmap, or network, of 1-dimensional curves, [2]. Roadmap methods have proven to be useful when considering vehicles subject to *kinodynamic* constraints. A kinodynamically constrained vehicle is subject to simultaneous kinematic and dynamic constraints, [8]. Roadmap approaches have been applied to extensions of the classical planning problem, such as the collision avoidance of dynamic obstacles with known trajectories, [9]. Due to the computational difficulties encountered in many complete planning methods, a variety of sampling-based roadmap techniques has been developed, [2, 10, 11, 12]. Roadmap methods, generally, consider robots modeled as points in the workspace. Claims have been made stating that augmenting obstacles with the geometry of the vehicle allows for collision avoidance between the obstacle and robot geometries. Using this approach alone for rotating vehicles may result in certain planners that are overly conservative in approximating the obstacle space. Consequently, the planners are unable to effectively handle workspaces with narrow channels between obstacles. A number of techniques has been developed to successfully address the issue of nar-

row channels in roadmap methods. However, in expansive environments it becomes unlikely that the sampling based methods will select appropriate locations to model these channels, and, therefore, the success of these methods to handle the channel problem is limited to small workspaces. Roadmap methods address kinodynamic constraints by solving the motion planning problem in a higher dimensional space than the DOF of the system. Complete motion planning is likely to be exponential in the dimensionality of the problem, [12]. The sampling based roadmap techniques were developed to quickly and efficiently handle problems with high degrees of freedom, [11]. The trade off between the ability to solve these high dimensional problems is that proofs regarding reachability and controllability are not easily addressed and optimality cannot be guaranteed.

Cell decomposition techniques, like roadmap methods, preprocess the obstacle free subset of the workspace. These methods decompose the configuration space of the problem into convex regions referred to as *cells*. If the union of the void cells is exactly the configuration space, the decomposition is *exact*, [6]. An *approximate* cell decomposition refers to a decomposition in which the union of cells is a bounded approximation of the free space. These methodologies employ a configuration space approach, meaning they allow problems of motion planning for robots with convex geometries to be represented as motion planning problems of single points. After the decomposition has been obtained a connectivity graph, representing the adjacency relationships of the cells, is created [13]. The connectivity graph is then searched for a sequence of void cells, referred to as a *channel*, connecting the cell containing the initial configuration to the cell containing the goal configuration. Exact cell decompositions are complete, while approximate cell decompositions are *resolution complete*, as completeness is approached when the cells become infinitely small. These methods have the benefit, given appropriate resolutions, of addressing the narrow passage problem for rotating vehicles with geometries. Recently, cell decomposition

problems have been extended to account for the *treasure hunt*, or information-driven sensor management problem [13, 14], and the sensing and pursuit problem, [15]. The computation of decompositions and associated data structures can be expensive in time and memory, [1]. Furthermore, cell decomposition techniques are limited by the volume of the configuration space. This volume increases exponentially with the DOF of the vehicle, and, therefore, these approaches are intractable even for relatively small DOF problems, [3].

The final class of motion planning methods is referred to as *mathematical programming*. In these algorithms planning is complete, accomplished directly in the workspace, and requires no preprocessing, [16]. The subclass of mathematical programming called *mixed integer programming* (MIP) has been studied extensively due to its ability to adequately address convex obstacle avoidance and a variety of other constraints ranging from multi-vehicle collision avoidance, [17], to mobile router connectivity, [18]. MIP allows for the inclusion of both continuous and binary variables, giving it flexibility in modeling capabilities over alternative approaches. These techniques have been applied to problems involving autonomous underwater vehicles, [19], plume avoidance, [20], spacecraft trajectory planning, [21], air traffic management, [22], and cooperative robot control, [23]. The benefit of the MIP class of algorithms is that they are able to guarantee optimality and directly address optimal control considerations, [24]. Mixed integer programs have proven to be successful complete, [25], global optimization techniques for optimal control problems which minimize geometric and non-geometric costs. However, MIP methods suffer from a number of limitations. These approaches, due to how obstacles are addressed, are not able to handle workspaces with concave obstacles. Furthermore, MIP techniques have not been extended to account for rotating robots with geometries or kinodynamic constraints other than the double integrator kinematics, [17, 26]. Another major disadvantage of MIP is that solving these problems is NP-hard, there-

fore, computational requirements can grow dramatically with the number of binary variables, [27].

This thesis proposes a technique to extend the application of MIP to account for vehicle kinematics other than the double integrator. The method developed discretized the *unicycle* kinematic model in the form of a piece-wise linear time invariant system, such that it can be included in the final mixed integer program. In addition, the research presented introduces a combination of cell decomposition and MIP methodologies in order to take advantage of their strengths and avoid their weaknesses. In particular, it will show that this approach can simultaneously address nonholonomic vehicle constraints - a weakness of cell decomposition methods - and concave obstacles and vehicles capable of rotation - a limit of MIP techniques. The combination of these methods will also be able to address the problem of narrow passages in a large workspace, unlike potential field and roadmap methods. The methodology developed does not require kinodynamic problems to be considered in higher dimensional space. Therefore, it is suggested that the complexity of the method may not grow exponentially with the inclusion of kinodynamic constraints. However, complexity claims, at present, are limited to the discussion of the degree of the space the problem is solved in. Future work will study in detail the complexity of this approach. The method presented is able to solve for optimal control histories simultaneously with geometric workspace considerations. Traditionally, optimal control and geometric planning are handled in a hierarchical manner, [28, 29], in which a geometrically feasible path is found and then the optimal control relationships are used to smooth the path. Hierarchical approaches have yet to make strong claims regarding optimality and are most often incomplete techniques. This will be avoided by the combination of mixed integer programming and cell decomposition. Furthermore, the flexibility of the MIP will allow for future work to consider optimization functions other than distance or time, an extension of the standard motion problem

not readily addressed by the alternative techniques.

The thesis is outlined as follows. It will begin by defining, in detail, the optimal path planning problem considered. Chapter 3 and Chapter 5 will provide the necessary background on mixed integer programming and cell decomposition required to fully understand the solution method developed. The kinematic model of the robot is discussed in Chapter 4. This discussion includes the continuous and discrete kinematics of the vehicle, as well as the novel discretization of the kinematics in the form of mixed-integer constraints. The remainder of the methodology is found in Chapters 6 and 7, which describe the utilization of cell decomposition, the optimal control problem considered, and the final algorithm. These chapters are followed by the results in the form of numerical simulations and then by concluding statements.

2

Problem Definition and Assumptions

This thesis considers the problem of determining a cost-optimal, collision-free trajectory for a wheeled robot (similarly, vehicle) between prescribed initial and final configurations. In robotics literature, this paradigm is commonly referred to as the *find path* or [piano] *mover's* problem.

2.1 Preliminaries

Let $\mathcal{W} \subset \mathbb{R}^2$ denote a two-dimensional Euclidean workspace populated by n fixed, polygonal obstacles, $\mathcal{B}_1, \ldots, \mathcal{B}_n$, that are not necessarily convex. As is convention with the find path class of problems, the positions and geometries of the obstacles are assumed known *a priori*, [30]. The geometry of the robot, $\mathcal{A}$, is a closed and bounded subset of the workspace. Consider a Cartesian reference frame, $\mathcal{F}_\mathcal{A}$, embedded in the vehicle platform. This moving reference frame rotates and translates with $\mathcal{A}$, and has an origin that is coincident with the geometric center of the robot, see Fig. 2.1. By comparing the orientation of $\mathcal{F}_\mathcal{A}$ to the fixed Cartesian reference frame of the workspace, $\mathcal{F}_\mathcal{W}$, it is possible to determine the exact position of every point on $\mathcal{A}$ in $\mathcal{W}$. Accordingly, the configuration of the robot is fully defined, at time t, by the

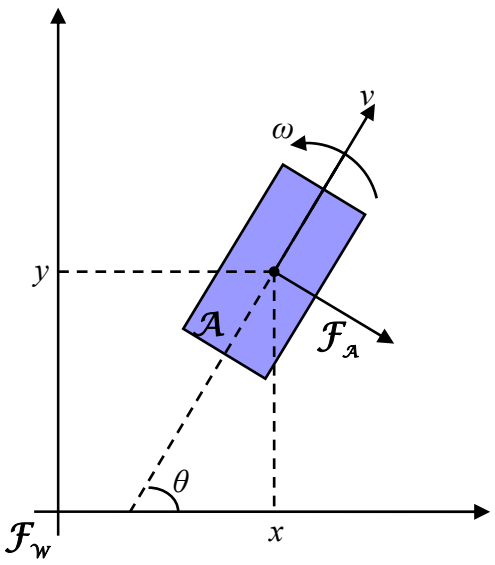

FIGURE 2.1: Geometry and associated reference frames of the robot

position of the origin of $\mathcal{F}_{\mathcal{A}}$, $(x(t),\ y(t))$, and the angle formed by the vertical axis of $\mathcal{F}_{\mathcal{A}}$ and the horizontal axis of $\mathcal{F}_{\mathcal{W}}$, $\theta(t)$, as diagrammed in Fig. 2.1. The vector created by the position and orientation of the robot in $\mathcal{W}$ is referred to as the *state* of the system, denoted by $\mathbf{x}(t) = [x(t),\ y(t),\ \theta(t)]^{\mathrm{T}}$. The orientation angle of the vehicle, $\theta(t)$, is restricted to the range $\Theta = [\theta_{min}, \theta_{max}]$. The optimization problem must consider simultaneous movement of the centroid of the robot in $\mathcal{W}$ and the rotation of its geometry in Θ. For this reason, the methodology developed in this thesis is presented for, without loss of generality, $\mathcal{C} = \mathcal{W} \times \Theta$, where $\mathcal{C}$ designates the *configuration space* of the vehicle.

Definition 1. *The* ***configuration space*** *is the space of all possible position and orientation pairs of a vehicle, $\mathcal{A}$, in a workspace, $\mathcal{W}$, [6].*

Due to the presence of obstacle, not all robot configurations in $\mathcal{W}$ are free from collisions. The following section describes how to obtain the subset of $\mathcal{C}$, called the *free configuration space*, $\mathcal{C}_{free}$, that contains only the collision free states of the vehicle.

2.2 C-Obstacles and the Free Configuration Space

As previously stated, the geometry of the robot is a closed and bounded subset of the workspace, $\mathcal{W}$. In order to determine the free configuration space, $\mathcal{C}_{free}$, of the robot, *C-obstacles* must first be calculated for all workspace obstacles.

Definition 2. *A* ***C-obstacle****, $\mathcal{CB}_j$, is a subset of the configuration space that, if entered by a representative point of the robot (e.g. centroid), will cause a collision between the geometry of $\mathcal{A}$ and the obstacle $\mathcal{B}_j$.*

When the vehicle has state $\mathbf{x}$, the subset of the workspace occupied by the geometry of the robot is denoted by $\mathcal{A}(\mathbf{x})$. The C-obstacle of $\mathcal{B}_j$ is a closed region in $\mathcal{W}$ obeying the following

$$\mathcal{CB}_j = \{\mathbf{x} \in \mathcal{C} / \mathcal{A}(\mathbf{x}) \cap \mathcal{B}_j \neq \emptyset\} \tag{2.1}$$

The union of all C-obstacles, $\bigcup_{j=1}^{n} \mathcal{CB}_j$, is referred to as the *C-obstacle region*. By the above definitions, the free configuration space, $\mathcal{C}_{free}$, is formally defined as

$$\mathcal{C}_{free} = \mathcal{C} / \bigcup_{j=1}^{n} \mathcal{CB}_j = \left\{ \mathbf{x} \in \mathcal{C} / \mathcal{A}(\mathbf{x}) \cap \left(\bigcup_{j=1}^{n} \mathcal{B}_j \right) \neq \emptyset \right\} \tag{2.2}$$

C-obstacles, and, consequently, $\mathcal{C}_{free}$, can be easily computed for the case of a translating robot (i.e. $\mathcal{C} = \mathcal{W}$). This is because the C-obstacles correspond to a simple augmentation of the obstacle geometries with the geometry of the robot. An example of the latter augmentation is found in see Fig. 2.2(a). When the robot is capable of rotating, (i.e. $\mathcal{C} = \mathcal{W} \times \Theta$), C-obstacles will differ with each robot orientation angle. For this reason, computing $\mathcal{C}_{free}$ becomes more complex when vehicle rotation is considered as compared to translation alone. Fig. 2.2(a) and Fig. 2.2(b) show the C-obstacles associated with the same obstacle and two different robot orientation angles. Considering the aforementioned relationship between $\mathcal{CB}_j$

and the robot orientation, when the vehicle is capable of rotating, C-obstacles become three-dimensional subsets of $\mathcal{C}$, as shown in Fig. 2.2(c).

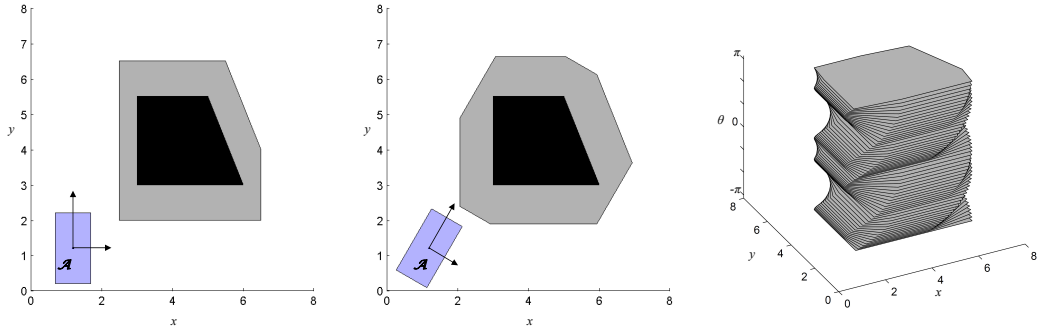

(a) C-Obstacle for $\theta = \pi$ (b) C-Obstacle for $\theta = \pi/3$ (c) C-Obstacle in 3D

FIGURE 2.2: C-Obstacles

In order to address the complexity of three-dimensional C-obstacles, the rotation range, Θ, is discretized into intervals of length $\Delta\theta$. C-obstacles are then calculated for each interval, such that for any robot orientation angle contained in the interval the robot will not collide with the obstacles. This approach is referred to as *orientation slicing* and is outlined in [6]. The discretization of Θ via orientation slicing is a commonly implemented technique in cell decomposition methods to address three dimensional C-obstacles, [14].

2.3 The Optimal Control Problem

The algorithm developed in this these must determine an admissible set of control inputs, $\mathbf{u}(t)$, to transition the system from an initial state, $\mathbf{x}_{init}$, to a final state, $\mathbf{x}_{final}$, while obeying an optimal control policy. the model used in this research (Chapter 4 is such that the control inputs are the linear and angular velocities of the robot, denoted as $v(t)$ and $\omega(t)$, respectively. Therefore, the control vector is as follows $\mathbf{u}(t) = [v(t),\ \omega(t)]^{\mathrm{T}}$. For conciseness, from this point forward $\mathbf{x}$ and $\mathbf{u}$ will explicitly define the time dependent state and control vectors, i.e. $\mathbf{x} = \mathbf{x}(t)$.

This section will consider the general form for the relationship between the state and control vectors (see Eqn. 2.4). A detailed description of the state kinematics applied in this research can be found in Chapter 4.

The robot must navigate the workspace while obeying the kinematic model and minimizing (or maximizing) a given objective function. This minimization of the cost function, $J(\mathbf{x}, \mathbf{u})$, is in the form of the classical optimal control problem as shown below,

$$\min_{\mathbf{x},\mathbf{u}} \quad J(\mathbf{x}, \mathbf{u}) = \phi\left[\mathbf{x}(t_f), t\right] + \int_{t_0=0}^{t_f} \mathcal{L}\left[\mathbf{x}, \mathbf{u}, t\right] dt \tag{2.3}$$

$$\text{subject to:} \quad \dot{\mathbf{x}} = f\left[\mathbf{x}, \mathbf{u}, t\right] \tag{2.4}$$

where $\mathcal{L}[\cdot]$ defines the instantaneous cost of the trajectory, $\phi[\cdot]$ is a final state penalty, and t_f is the final time at which the final state is obtained. In this research, the optimal trajectory problem does not require a final state penalty, and is therefore an optimization function of the *Lagrange type*, [31]. In most practical motion planning applications, the instantaneous cost can be modeled as a linear or quadratic function of the state and control variables. Consequently, the integrand takes the following form

$$\mathcal{L}\left[\mathbf{x}, \mathbf{u}, t\right] = \mathbf{x}^{\mathrm{T}}\mathbf{Q}_c\mathbf{x} + \mathbf{u}^T\mathbf{R}_c\mathbf{u} \tag{2.5}$$

where $\mathbf{Q}_c$ and $\mathbf{R}_c$ are (semi-) positive definite weighting matrices with values that are determined based on the problem being studied. The subscript c, in the equation above, denotes the continuous time representation of the system. In the literature, instantaneous trajectory costs in the form of Eqn. 2.5 have been used to model a variety of objectives, including minimization of fuel consumption and target tracking.

The value of t_f is unknown, as a result most trajectory problems of the Lagrange

type are considered over infinite time ranges,

$$\min_{\mathbf{x},\mathbf{u}} \quad J(\mathbf{x},\mathbf{u}) = \int_0^\infty \left(\mathbf{x}^{\mathrm{T}}\mathbf{Q}\mathbf{x} + \mathbf{u}^{\mathrm{T}}\mathbf{R}\mathbf{u}\right) dt \tag{2.6}$$

$$\text{subject to:} \quad \dot{\mathbf{x}} = \mathbf{A}_c\mathbf{x} + \mathbf{B}_c\mathbf{u} \tag{2.7}$$

As a way to simplify numerical computations, the majority of solution methods determine optimal trajectories over a finite time frame, i.e. $t \in [0, T]$, where T is a *finite horizon time*. Eqn. 2.6 becomes,

$$\min_{\mathbf{x},\mathbf{u}} \quad J(\mathbf{x},\mathbf{u}) = \int_0^T \left(\mathbf{x}^{\mathrm{T}}\mathbf{Q}_c\mathbf{x} + \mathbf{u}^{\mathrm{T}}\mathbf{R}_c\mathbf{u}\right) dt \tag{2.8}$$

The algorithm must solve for the set of control inputs, $\mathbf{u}$ for $t \in [0, T]$, needed to achieve the goal configuration $\mathbf{x}_{final}$, while obeying Eqn. 2.7, optimizing Eqn. 2.8, and beginning in a prescribed initial state, i.e. $\mathbf{x}(t = 0) = \mathbf{x}_{init}$.

In order to solve the aforementioned control problem numerically, the system must be discretized in time. The finite horizon time is divided into N steps of length Δt, i.e. $\Delta t = \frac{T}{N}$. Let the subscripts $k \in [0, \ldots, N]$ denote discrete time variables, such that $\mathbf{x}_k = \mathbf{x}(t = k\Delta t)$ and $\mathbf{u}_k = \mathbf{u}(t = k\Delta t)$. In discrete time, Eqn. 2.7 becomes

$$\mathbf{x}_{k+1} = \mathbf{A}_d\mathbf{x}_k + \mathbf{B}_d\mathbf{u}_k \tag{2.9}$$

where the subscript d indicates the discrete system.

In this thesis, the algorithm must return a distance optimal path between the initial and final configurations. The distance optimization is approximated by the square of the L_2 norm of the discrete state variables,

$$J(\mathbf{x}) = \sum_{k=1}^{N} (\mathbf{x}_k - \mathbf{x}_{k-1})^{\mathrm{T}} (\mathbf{x}_k - \mathbf{x}_{k-1}) \tag{2.10}$$

The final, discrete time optimization is as follow,

$$\min_{\mathbf{x},\mathbf{u}} \quad J(\mathbf{x}) = \sum_{k=1}^{N} (\mathbf{x}_k - \mathbf{x}_{k-1})^{\mathrm{T}} (\mathbf{x}_k - \mathbf{x}_{k-1}) \tag{2.11}$$

$$\text{subject to:} \quad \mathbf{x}_{k+1} = \mathbf{A}_d\mathbf{x}_k + \mathbf{B}_d\mathbf{u}_k \tag{2.12}$$

This research aims to develop an appropriate set of constraints such that the optimal control problem above can be solved for a collision free kinematically feasible path.

3

Background on Disjunctive Programming

Disjunctive programming is a technique implemented in a variety of fields, from economics to engineering, to effectively model and solve large, constrained optimizations that involve both algebraic and logical constraints. In these problems, a cost function, $J(\mathbf{x})$, is minimized over a set of state variables, $\mathbf{x}$, which is subject to constraints that are *conjunctions*, $\bigwedge$ = AND, of n clauses, where each clause is a *disjunction*, $\bigvee$ = OR, of m_i inequality constraints. Accordingly, a disjunctive program (DP) has the following general form

$$\begin{aligned} \min_{\mathbf{x}} \quad & J(\mathbf{x}) \\ \text{subject to:} \quad & \bigwedge_{i=1:n} \left(\bigvee_{j=1:m_i} C_{ij}(\mathbf{x}) \leq 0 \right) \end{aligned} \tag{3.1}$$

Although disjunctive programming is a powerful tool for modeling a variety of optimization problems, DPs are not always readily implemented in mathematical optimization software. As a result, DPs are commonly reformulated as mixed integer programs (MIP), which are easily solved by commercially available programs, such as CPLEX, [32]. The aforementioned transformation of DPs into equivalent MIPs is

described in the following section.

3.1 Mixed Integer Programming

As explained in the previous section, DPs must be redefined as equivalent MIPs. Unlike DPs, which contain logical and algebraic constraints on the system variables, MIPs contain algebraic constraints that involve both the system variables and a set of integer *decision variables*. In this research, these additional integer variables are binary, i.e. they can only have the value of 0 or 1. Let the literal X_i represent a constraint statement for $\mathbf{x}$. In the DP framework, each X_i is associated with a logical value, i.e. either TRUE or FALSE. Consider instead associating each X_i with a binary decision variable, δ^i. The logical relationships between different constraints in the DP can be written by equivalent algebraic constraints on the decision variables, as shown below

$$\begin{array}{rll} X_1 \text{ AND } X_2 & \text{is equivalent to} & \delta^1 = 1,\ \delta^2 = 1 \\ X_1 \text{ OR } X_2 & \text{is equivalent to} & \delta^1 + \delta^2 \geq 1 \\ \text{NOT}(X_1) & \text{is equivalent to} & \delta^1 = 0 \\ X_1 \rightarrow X_2 & \text{is equivalent to} & \delta^1 - \delta^2 \leq 0 \\ X_1 \leftrightarrow X_2 & \text{is equivalent to} & \delta^1 - \delta^2 = 0 \\ X_1 \oplus X_2 & \text{is equivalent to} & \delta^1 + \delta^2 = 1 \end{array}$$

The well known *big M* theory, [18], can be used to establish direct connections between the constraints on the binary decision variables and the system variables. Consider the following linear constraint and associated decision variable, δ^i,

$$X_i : \quad a_i^{\mathrm{T}}\mathbf{x} \leq b_i \tag{3.2}$$

When $\delta^i = 1$, the constraint in Eqn. 3.2 is applied to $\mathbf{x}$, and, conversely, when $\delta^i = 0$ the constraint does not hold. Then, by implementing big M theory, the relationship between δ^i and Eqn. 3.2 can be written as the following linear mixed integer constraint

$$a_i^{\mathrm{T}}\mathbf{x} \leq b_i + M(1 - \delta^i) \tag{3.3}$$

where M is a large positive number. Once again, when $\delta^i = 1$ the constraint in Eqn. 3.2 holds. If $\delta^i = 0$, the constraint becomes $a_i^{\mathrm{T}}\mathbf{x} \leq b_i + M$. The assumption of big M theory is that $a_i^{\mathrm{T}}\mathbf{x}$ will always be less than M, and, therefore, the latter inequality is equivalent to no constraint being applied to $\mathbf{x}$. Thus, the linear mixed integer constraint of Eqn. 3.3 retains the relationship between the decision variables and the algebraic constraint of Eqn. 3.2.

Big M theory is easily extended to account for disjunctions of multiple constraints. Consider two constraints, X_i and X_j, with a disjunction between them, i.e. $X_i \bigoplus X_j$, the following mixed integer constraints hold,

$$a_i^{\mathrm{T}}\mathbf{x} \leq b_i + M(1 - \delta^i) \tag{3.4}$$

$$a_j^{\mathrm{T}}\mathbf{x} \leq b_j + M(1 - \delta^j) \tag{3.5}$$

$$\delta^i + \delta^j = 1 \tag{3.6}$$

The above set of equations enforces the original disjunction on the constraints. As exhibited above, big M theory is a powerful method for reformulating DPs as analogous MIPs.

3.2 Piece-Wise Linear Time Invariant Systems

Mixed logical dynamical (MLD) systems constitute a subset of dynamic systems in which the dynamic (or kinematic) components are governed by logical constraints. This section investigates a special case of MLD systems, referred to as piece-wise linear time invariant (PWLTI) systems.

A PWLTI system is a set of dynamic cases, such that at a given time step, k, only one of the m possible dynamic relationships is true. The general form of a PWLTI

system, [33], for the discrete state and control vectors, $\mathbf{x}_k$ and $\mathbf{u}_k$, is defined as,

$$\mathbf{x}_{k+1} = \begin{cases} A^1\mathbf{x}_k + B^1\mathbf{u}_k & \text{if } \delta_k^1 = 1 \\ \vdots & \vdots \\ A^j\mathbf{x}_k + B^j\mathbf{u}_k & \text{if } \delta_k^j = 1 \\ \vdots & \vdots \\ A^m\mathbf{x}_k + B^m\mathbf{u}_k & \text{if } \delta_k^m = 1 \end{cases} \tag{3.7}$$

where δ_k^j is a binary decision variable associated with the respective kinematic statement, $j \in [1, \ldots, m]$, at time step $k \in [0, \ldots, N-1]$. Furthermore, the decision variables must satisfy the following exclusive-or condition,

$$\bigoplus_{j=1}^{m} \delta_k^j = 1 \tag{3.8}$$

The condition above guarantees that only one of the dynamic statements in Eqn. 3.7 is true at a particular time step.

The PWLTI system defined above can be easily reformulated as a set of mixed integer constraints using big M theory. Accordingly, Eqn. 3.7 and Eqn. 3.8 become

$$\forall\ j \in [1, \ldots, m]$$

$$\mathbf{x}_{k+1} \leq A^j\mathbf{x}_k + B^j\mathbf{u}_k + M(1 - \delta_k^j) \tag{3.9}$$

$$\mathbf{x}_{k+1} \geq A^j\mathbf{x}_k + B^j\mathbf{u}_k - M(1 - \delta_k^j) \tag{3.10}$$

$$\sum_{j=1}^{m} \delta_k^j = 1 \tag{3.11}$$

The pair of inequality above become a single equality constraint for when $\delta_k^j = 1$, and, therefore, retain the properties of the original PWLTI system.

3.2.1 Controllability of PWLTI Systems

A MLD system is controllable if an admissible sequence of control inputs exist to transition the system from an initial state to a desired final state (both of which

must be valid components of the state space of the system), [34]. Importantly, the controllability of MLD systems cannot be determined from the controllability of the component subsystems. Due to issues associated with computational complexity, analyzing the controllability of MLD systems is most often accomplished using numerical verification.

3.3 Obstacle Avoidance

Consider a translating robot, i.e. $\mathbf{x} = [x,\ y]^{\mathrm{T}}$, with geometry $\mathcal{A}$, in an obstacle populated environment. The C-obstacles are two dimensional subsets of the configuration space. Let e_{ij} denote the j-th edge of C-obstacle $\mathcal{CB}_i$. There exists a two dimensional hyperplane, h_{ij}, that is collinear with e_{ij}, as seen in Fig. 3.1, where

$$h_{ij}: \quad a_{ij}^{\mathrm{T}}\mathbf{x} = b_{ij} \tag{3.12}$$

Let s_{ij} be the half-space that is defined by h_{ij}, which does not contain $\mathcal{CB}_i$,

$$s_{ij}: \quad a_{ij}^{\mathrm{T}}\mathbf{x} \leq b_{ij} \tag{3.13}$$

The robot will avoid collisions with obstacle $\mathcal{B}_i$ if its centroid is contain in any of the half-spaces s_{ij}, corresponding to the associated C-obstacle $\mathcal{CB}_i$. This condition is expressed below,

$$\bigvee_{j=1:|\mathcal{CB}_i|} a_{ij}^{\mathrm{T}}\mathbf{x} \leq b_{ij} \tag{3.14}$$

where $|\mathcal{CB}_i|$ is the number of sides of $\mathcal{CB}_i$. When $C_{ij}(\mathbf{x}) = a_{ij}^{\mathrm{T}}\mathbf{x} - b_{ij}$, the above equation can be written equivalently as

$$\bigvee_{j=1:|\mathcal{CB}_i|} C_{ij}(\mathbf{x}) \leq 0 \tag{3.15}$$

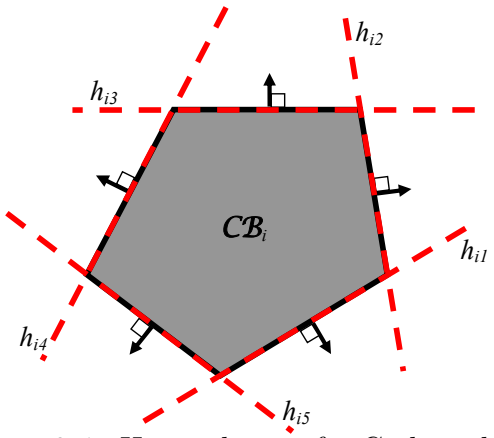

FIGURE 3.1: Hyperplanes of a C-obstacle, $\mathcal{CB}_i$

In order for the vehicle to avoid collisions with all obstacles in the workspace, the following conjunction must hold,

$$\bigwedge_{i=1:n} \bigvee_{j=1:|\mathcal{CB}_i|} C_{ij}(\mathbf{x}) \leq 0 \tag{3.16}$$

The set of constraints above must be satisfied at every point on the trajectory of a robot to guarantee collision avoidance.

The above disjunctive methodology has been used in literature to effectively address obstacle avoidance for translating, point-like robots, [17, 35, 20]. However, the hyperplane formulation is not easily extended to account for three-dimensional C-obstacles, and, ergo, robots capable of rotation. Furthermore, this technique fails when obstacles are concave. Consider the concave obstacle in Fig. 3.2 and the half-spaces defined by h_{i1} and h_{i2}. Due to the shape of the obstacle, h_{i1} and h_{i2} produce conflicting constraints. For instance, if the robot was in the half-space defined by h_{i1}, it could potential collide with the obstacle in the shaded region. In order to avoid the limitations of existing disjunctive programming approaches, this thesis develops a novel technique that implements disjunctions on the free-configuration space of the vehicle, as opposed to disjunctions on the C-obstacle region. This will allow the methodology to address both concave obstacles and rotating vehicles.

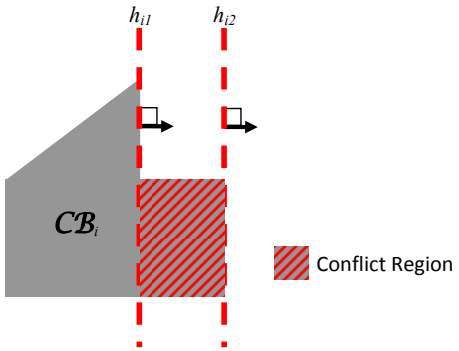

FIGURE 3.2: Conflict Region for a Concave Obstacle

4

The Unicycle Model

This chapter presents a novel discretization of the vehicle kinematics in the form of a piece-wise linear time invariant (PWLTI) system. Chapter 2 has shown that PWLTI systems can be easily included in mixed integer programs (MIP). The technique below constructs a set of linear mixed integer constraints that effectively approximate the nonlinear, time invariant system kinematics of the vehicle.

The maneuverability of the robot is defined by the unicycle kinematics. The state of the robot is given by the position and orientation of the vehicle $\mathbf{x} = [x,\ y,\ \theta]^{\mathrm{T}}$, and the instantaneous linear and angular velocities of the vehicle constitute the control vector, $\mathbf{u} = [v,\ \omega]^{\mathrm{T}}$. Where both $\mathbf{x}$ and $\mathbf{u}$ are functions of time. In the unicycle model, the time derivatives of the state variables cannot take independent values. Rather, the state variables, their derivatives, and the control variables are related through the following set of equations.

$$\dot{x} = v\cos\theta \tag{4.1}$$

$$\dot{y} = v\sin\theta \tag{4.2}$$

$$\dot{\theta} = \omega \tag{4.3}$$

Formally, the statements above mathematically define the unicycle kinematics. This model is commonly referred to as a *kinematic* relationship, as it does not address the forces or torques on the robot, [36]. Using a vector notation, Eqn. 4.1 - 4.3 can be written more concisely as

$$\dot{\mathbf{x}} = \begin{bmatrix} \cos\theta & 0 \\ \sin\theta & 0 \\ 0 & 1 \end{bmatrix} \mathbf{u} \tag{4.4}$$

Eqn. 4.4 is commonly referred to as the state equation.

In the unicycle model, the linear velocity of the vehicle is always along its main axis. This condition can be expressed as follow

$$\dot{x}\sin\theta - \dot{y}\cos\theta = 0 \tag{4.5}$$

In robotics literature, this relationship is referred to as the *no-slip condition*, [37]. Physically, this means that the vehicle can only move in the direction that its wheels face. This assumption is a well established limitation of wheeled vehicles in moderate speed scenarios, [38]. The no-slip condition is a *nonholonomic constraint* on the system variables.

Definition 3. *A **nonholonomic constraint**, [6], is a non-integrable equality constraint that is a function of the state variables of a system and their derivatives.*

The controllability of vehicles with nonholonomic kinematics is investigated in [39]. In summary, it was found that a robot governed by a single nonholonomic equality constraint is *fully controllable*, [6]. A vehicle is fully controllable if it is able to follow any collision free path in $\mathcal{W}$. By these definitions, a robot with unicycle kinematics is fully controllable.

4.1 Temporal Discretization

The trajectory problem must be discretized in time so that a numerical solution can be computed. This research implements a first order, Euler discretization of the continuous kinematics found in Eqn. 4.1 - 4.3, where Δt and k are identical to those defined in Chapter 2. The unicycle model in discrete time is given by

$$x_{k+1} = x_k + \Delta t \ (v_k \cos\theta_k) \tag{4.6}$$

$$y_{k+1} = y_k + \Delta t \ (v_k \sin\theta_k) \tag{4.7}$$

$$\theta_{k+1} = \theta_k + \Delta t \ \omega_k \tag{4.8}$$

Using vector notation the above equations can be written as

$$\mathbf{x}_{k+1} = \begin{bmatrix} 1 & 0 & 0 \\ 0 & 1 & 0 \\ 0 & 0 & 1 \end{bmatrix} \mathbf{x}_k + \begin{bmatrix} \Delta t \ (\cos\theta_k) & 0 \\ \Delta t \ (\sin\theta_k) & 0 \\ 0 & \Delta t \end{bmatrix} \mathbf{u}_k \tag{4.9}$$

The first-order Euler approximation is a useful and easily computed temporal discretization, however, it is a temporally linear discretization and is therefore only valid over short time intervals. Therefore, discretion must be used when selecting the values for Δt, N, and T for a particular system.

4.2 PWLTI Angular Discretization

The MIP optimization software used in this research, Tomlab/CPLEX, is most effectively utilized in problems where the mixed integer constraints are linear. Although nonlinear programming packages are available, the computational requirements of solutions for nonlinearly constrained MIPs are numerically demanding. The unicycle model, even in discrete time, is nonlinear in θ_k due to the no-slip condition. Therefore, it is necessary to approximate Eqn. 4.9 by a set of linear equations. This is accomplished by use of the PWLTI framework described in Chapter 3.

First, the range of all possible robot rotation angles, $\Theta = [\theta_{min}, \theta_{max}]$, is divided into m equally sized, non-overlapping intervals $[\phi^0, \phi^1], \ldots, [\phi^{m-1}, \phi^m]$, where $\phi^0 = \theta_{min}$ and $\phi^m = \theta_{max}$. Consider the j-th interval $[\phi^{j-1},\ \phi^j]$, for $j \in [1, \ldots, m]$ and

$$\phi^j = \frac{\theta_{max} - \theta_{min}}{m} j \tag{4.10}$$

$$\phi^j_{mid} = \frac{\theta_{max} - \theta_{min}}{m} \left(j - \frac{1}{2} \right) \tag{4.11}$$

where ϕ^j_{mid} is the midpoint of the interval. If the interval $[\phi^{j-1},\ \phi^j]$ is small enough, it is assumed that for $\theta_k \in [\phi^{j-1},\ \phi^j]$ the dynamics in Eqn. 4.9 can be approximated by the following

$$\mathbf{x}_{k+1} = \begin{bmatrix} 1 & 0 & 0 \\ 0 & 1 & 0 \\ 0 & 0 & 1 \end{bmatrix} \mathbf{x}_k + \begin{bmatrix} \Delta t\ (\cos \phi^j_{mid}) & 0 \\ \Delta t\ (\sin \phi^j_{mid}) & 0 \\ 0 & \Delta t \end{bmatrix} \mathbf{u}_k \tag{4.12}$$

Eqn. 4.12 is a linear time invariant approximation of the kinematics for $\theta_k \in [\phi^{j-1},\ \phi^j]$. This relationship can be implemented as a set of mixed integer linear constraints over the entire rotation range, Θ, and used to approximate the unicycle

kinematics. The approximation of the kinematic model is as follows

$$\forall\ j \in [1, \ldots, m]$$

$$\mathbf{x}_{k+1} \leq A^j \mathbf{x}_k + B^j \mathbf{u}_k + M(1 - \delta_k^j) \tag{4.13}$$

$$\mathbf{x}_{k+1} \geq A^j \mathbf{x}_k + B^j \mathbf{u}_k - M(1 - \delta_k^j) \tag{4.14}$$

$$A^j = \begin{bmatrix} 1 & 0 & 0 \\ 0 & 1 & 0 \\ 0 & 0 & 1 \end{bmatrix} \tag{4.15}$$

$$B^j = \begin{bmatrix} \Delta t \ \cos\phi_{mid}^j & 0 \\ \Delta t \ \sin\phi_{mid}^j & 0 \\ 0 & \Delta t \end{bmatrix} \tag{4.16}$$

$$\theta_k \leq \phi^j + M(1 - \delta_k^j) \tag{4.17}$$

$$\theta_k \geq \phi^{j-1} - M(1 - \delta_k^j) \tag{4.18}$$

$$\sum_{j=1}^{m} \delta_k^j = 1 \tag{4.19}$$

These equations are in the form of the mixed integer representation of the general PWLTI system. The discretization of the nonholonomic unicycle kinematics in the form of a PWLTI system is a novel approach developed in this research for a rotating robot.

5

Background on Approximate Cell Decomposition

Cell decomposition is a well established class of solution methods for robotic path planning in obstacle populated environments. The primary step of these algorithms is to decompose the free configuration space, $\mathcal{C}_{free}$, into a set, $\mathcal{K}_{void}$, of empty (i.e. conflict free), convex regions called *cells*. Cell decomposition methods are categorized as either *exact* or *approximate*. In exact cell decomposition (ECD), the union of the void cells is *exactly* the free configuration space of the robot, i.e. $\cup\mathcal{K}_{void} = \mathcal{C}_{free}$. ECD has been studied in detail as it is a *complete* planning method. However, obtaining an ECD of a workspace is not always a computationally realistic procedure as the complexity of obtaining such a decomposition grows drastically with workspace dimension and size. As a result, ECD is commonly restricted to the set of problems containing planar or convex polyhedral obstacles [40, 41, 42, 43], and vehicles capable of translation only.

Approximate cell decomposition (ACD) algorithms result in a set of convex, non-overlapping polygons of a predefined shape. In these methods, $\mathcal{K}_{void}$ is a conservative representation of the free space. Therefore, the union of cells in $\mathcal{K}_{void}$ which form a bounded approximation of the free configuration space, i.e. $\cup\mathcal{K}_{void} \subseteq \mathcal{C}_{free}$. As is

the case with exact cell decomposition, ACD can be accomplished using a variety of techniques. This research implements a *quadtree* approach to ACD, in which the free configuration space is decomposed into cells with square projections on the $x-y$ plane, [44]. Alternative techniques, such as the *approximate-and-decompose* method, [45], that decomposes $\mathcal{C}_{free}$ into *rectangloid* cells, have been successfully implemented for similar motion planning problems, [14, 46, 15].

5.1 Quadtree Decomposition

Quadtrees are hierarchical data structures that are used to partition two-dimensional spaces, [47]. They are frequently implemented as a way to approximately decompose the void configuration space in obstacle populated environments, [44]. For each C-obstacle space obtained by orientation slicing a decomposition was computed using the quadtree approach, [6]. The algorithm work by recursively dividing the workspace into cells and labeling these cells as FULL, EMPTY or MIXED. A cell is characterized as FULL if its interior is completely contained in a C-obstacle, as EMPTY if its interior intersects no C-obstacles, and as MIXED otherwise. The technique begins by dividing the workspace into four quadrants, which are then labeled. If a cell is FULL the algorithm does nothing. Cells labeled EMPTY are added to the set of void cells, $\mathcal{K}_{void}$. If a cell is MIXED, it is divided into four equally sized quadrants, which are then labeled and stored, ignored, or divided accordingly. The quadtree decomposition recursively divides MIXED cells until a minimum cell size, or *resolution*, is reached. When the algorithm terminates, the set of empty cells, $\mathcal{K}_{void}$, is returned.

Each cell, κ^i, represents a closed and bounded subset of $\mathcal{C}_{free}$ defined by the limits $\kappa^i = [x^i_{min},\ x^i_{max}] \times [y^i_{min},\ y^i_{max}] \times [\theta^i_{min},\ \theta^i_{max}]$, as seen Fig. 5.1. The angular limits of the cell $[\theta^i_{min}, \theta^i_{max}]$, are defined in orientation approach used to address the issue of three dimensional C-obstacles. The dimensions of a cell κ^i, $(x^i_{max} - x^i_{min})$, $(y^i_{max} - y^i_{min})$, and $(\theta^i_{max} - \theta^i_{min})$, can be made arbitrarily small by adjusting the

resolution limits of the quadtree decomposition. However, applying finer resolutions increases the running time of the path planning algorithm. Therefore, a trade off exists between the precision of the approximation and the completeness of the solution. As a result, ACD methods are often called *resolution complete*, [6].

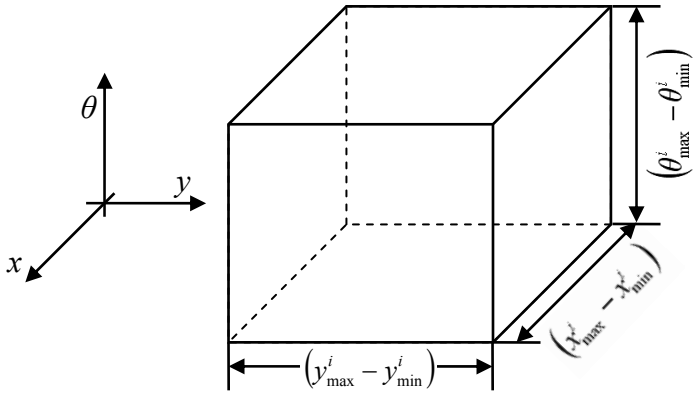

FIGURE 5.1: Geometry of cell κ^i

5.2 The Connectivity Graph

A primary assumption of the find path problem is that the robot moves continuously through the workspace. In a decomposed environment it can be shown that the assumption of a continuous path leads to the following claim: a robot is only capable of moving from the cell containing its current orientation to the set of geometrically adjacent cells or staying in its current cell. Let $int(R1, R2)$ indicate the intersection of the rectangles defined by $R1$ and $R2$. *Adjacency* is defined for two cells, $\kappa^i = [x^i_{min},\ x^i_{max}] \times [y^i_{min},\ y^i_{max}] \times [\theta^i_{min},\ \theta^i_{max}]$ and $\kappa^j = \left[x^j_{min},\ x^j_{max}\right] \times \left[y^j_{min},\ y^j_{max}\right] \times \left[\theta^j_{min},\ \theta^j_{max}\right]$, if one of the following is true [14],

1. The $int\left(\left[x^i_{min},\ x^i_{max}\right] \times \left[y^i_{min},\ y^i_{max}\right], \left[x^j_{min},\ x^j_{max}\right] \times \left[y^j_{min},\ y^j_{max}\right]\right)$ projected onto the $x - y$ plane is greater than zero, and $[\theta^i_{min}, \theta^i_{max}] \cap \left[\theta^j_{min}, \theta^j_{max}\right] \neq \emptyset$, Fig. 5.2(a).

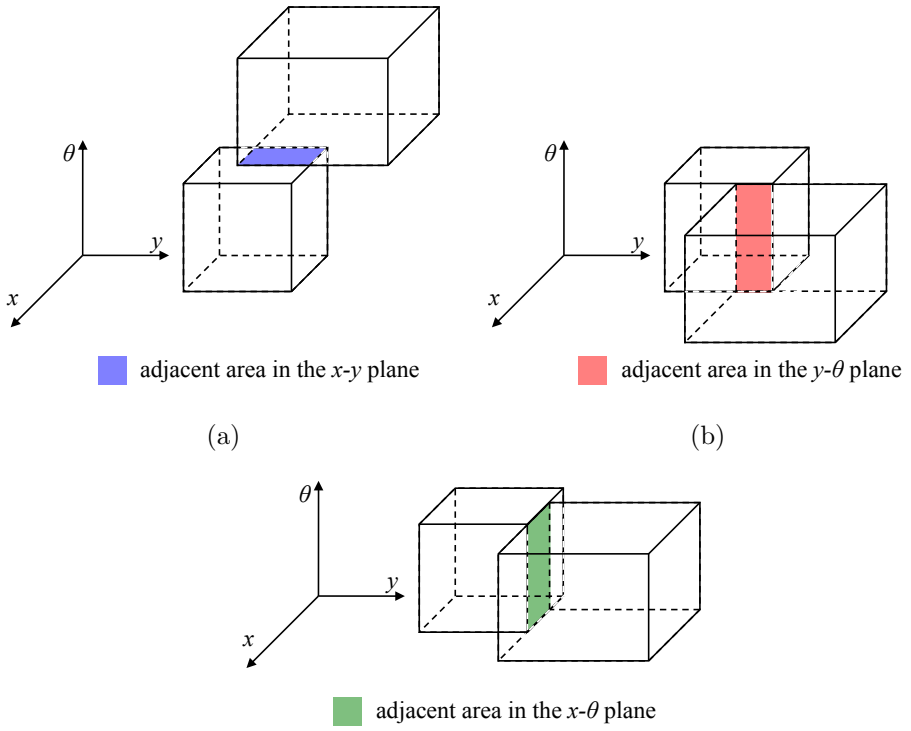

FIGURE 5.2: Adjacency Relationships for Various Cell Orientations

2. The $int\left(\left[y^i_{min},\ y^i_{max}\right] \times \left[\theta^i_{min},\ \theta^i_{max}\right], \left[y^j_{min},\ y^j_{max}\right] \times \left[\theta^j_{min},\ \theta^j_{max}\right]\right)$ projected onto the $y - \theta$ plane is greater than zero, and $[x^i_{min}, x^i_{max}] \cap \left[x^j_{min}, x^j_{max}\right] \neq \emptyset$, Fig. 5.2(b).

3. The $int\left(\left[x^i_{min},\ x^i_{max}\right] \times \left[\theta^i_{min},\ \theta^i_{max}\right], \left[x^j_{min},\ x^j_{max}\right] \times \left[\theta^j_{min},\ \theta^j_{max}\right]\right)$ projected onto the $x - \theta$ plane is greater than zero, and $[y^i_{min}, y^i_{max}] \cap \left[y^j_{min}, y^j_{max}\right] \neq \emptyset$, Fig. 5.2(c).

The adjacency relationships of a workspace can be defined concisely in a *connectivity graph.*

Definition 4. *A* ***connectivity graph****, $\mathcal{G}$, is an undirected graph, where vertices represent void cells and edges correspond to adjacency relationships of the cells. An edge, (κ^i, κ^j), exists in $\mathcal{G}$ connecting vertices κ^i and κ^j if and only if the respective*

cells are adjacent in $\mathcal{K}_{void}$, [14].

For pictorial simplicity, consider the two dimensional, decomposed workspace found in Fig. 5.3. By application of the adjacency definitions above, the connectivity graph for Fig. 5.3 was easily determined. It is found in Fig. 5.4.

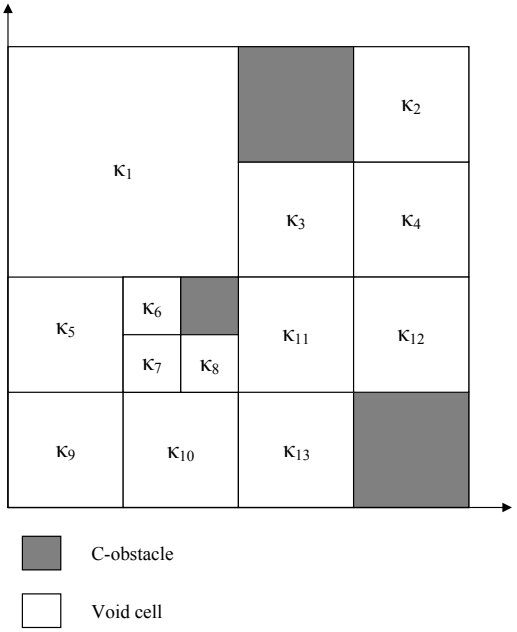

FIGURE 5.3: Example - Decomposed Workspace, $\mathcal{K}_{void}$

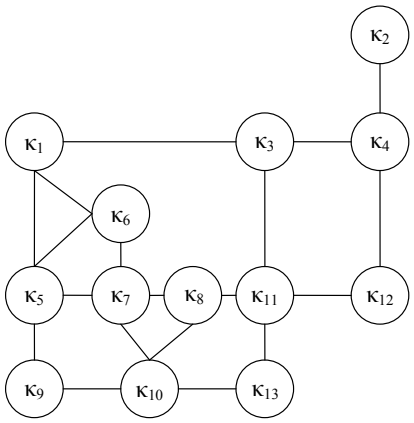

FIGURE 5.4: Example: Connectivity Graph, $\mathcal{G}$

In classical path planning algorithms that implement ACD, the solution method is four-fold. First, the workspace is decomposed into a set of collision-free cells, $\mathcal{K}_{void}$, using some form of ACD. Then the adjacency relationships are used to construct the connectivity graph, $\mathcal{G}$, of the workspace. The connectivity graph is then searched for a sequence of cells connecting the κ^{init}, the cell containing the initial configuration, and κ^{final}, the cell containing the goal configuration. These sequences of void cells are referred to as *channels*. Finally, when a void channel between κ^{init} and κ^{final} is found (using a graph searching technique) the path planning method concludes by determining a feasible path within the channel. The research presented in this thesis does not search the connectivity graph directly, rather, it transforms $\mathcal{G}$ into a directed graph called the *connectivity tree*, as outlined in Chapter 6.

6

The Connectivity Tree

Many methods have been devloped to search connectivity graphs for channels containing distance optimal collision free paths. This research implements a *connectivity tree* approach, similar to that outlined in [14] and [13]. In these articles, the authors use tree graphs to reduce the number of channels explored between $\kappa^{init} \ni \mathbf{x}_0$ and $\kappa^{final} \ni \mathbf{x}_N$.

Definition 5. *A **connectivity tree**, $\mathcal{T}$, is a tree graph associated with $\mathcal{G}$, where κ^{init} is the root and κ^{final} is in the leaves of the tree. A connected path from the root to a leaf is referred to as a **branch** and represents a channel in $\mathcal{K}_{void}$ connecting κ^{init} to κ^{final}.*

Unfortunately, the span of a connectivity tree grows dramatically with its depth. In order to avoid the computational complexity associated with a large connectivity tree a *pruning algorithm* can be used to remove suboptimal, redundant and superfluous paths from $\mathcal{T}$, [14]. A pruning algorithm algorithm assigns a weight to each edge in $\mathcal{T}$, and removes suboptimal paths by application of the Bellman equation of optimality, [31].

Many pruning techniques are unable to consider kinematic feasibility in branch removal. Consequently, the robot is often unable to effectively traverse the workspace. The following section presents an initial methodology for retaining a larger number of kinematically feasible paths. Importantly, the pruning algorithm used was created so that the techniques developed in this research could be tested. At this stage of the investigation, no current claims have been made regarding the optimality of this pruning technique. However, future work on the pruning algorithm aims to address optimality and completeness concerns.

6.1 Entry Nodes and the Connectivity Tree

This approach introduces the concept of *entry nodes*. An entry node, η_{ij}, is a representative point for the adjacency relationship of two cells, κ^i and κ^j. The position of the node is selected such that it corresponds to the geometric center of the adjacent area of κ^i and κ^j. The node η_{ij} is used as an approximation of the location that a robot would pass through if it was to *enter* κ^j from κ^i; and, as expected, $\eta_{ij} = \eta_{ji}$.

For simplicity, once again, consider the decomposed workspace found in Fig. 5.3, and the corresponding connectivity graph, $\mathcal{G}$, in Fig. 5.4. Once a connectivity graph has been obtained for a workspace, determining the positions of the entry nodes is trivial. Then, the connectivity of the entry nodes must be determined. Entry nodes are connected in $\mathcal{K}_{void}$ if they are positioned on the boundary of the same cell. These relationships create a new connectivity graph, $\mathcal{G}^\eta$, for the entry nodes of the workspace as opposed to the cells. The node connectivity of the example workspace is shown in Fig. 6.1. An additional node is added to $\mathcal{G}^\eta$ corresponding to the initial configuration of the robot, and, as seen in Fig. 6.1, it is connected to the entry nodes associated with κ^{init}. Furthermore, the connectivity of the entry nodes of κ^{final} are not included.

In this newly created connectivity graph, $\mathcal{G}^\eta$, the arcs are assigned weights corre-

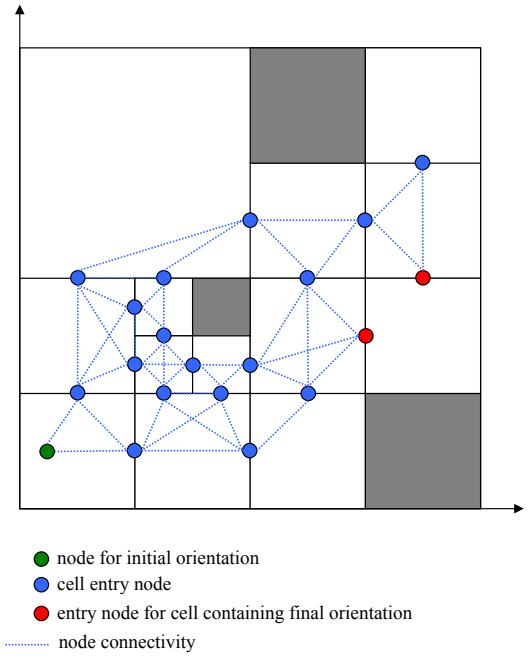

FIGURE 6.1: Example - Entry Node Connectivity, $\mathcal{G}^{\eta}$

sponding to the Euclidean distance between the nodes. *Dijkstra's algorithm*, [48, 49], can then be used to find optimal sequences of nodes, based on the associated connectivity weights, between the node corresponding to the initial configuration and the entry nodes of the final cell. Alternative graph searching methods to Dijkstra's algorithms, such as dynamic programming are available, however, as previously stated, the pruning algorithm is not the focus of this. Later work will investigate the variety of graphical methods available. The optimized connectivity graph, $\mathcal{G}^{\eta}_{opt}$, for the nodes in Fig. 6.1 is shown in Fig. 6.2. The graph, $\mathcal{G}^{\eta}_{opt}$, is then mapped back to the original void cells. This mapping leads to a pruned connectivity tree, $\mathcal{T}$, that will be used in determining the optimal trajectory. The final connectivity tree of the example workspace can be found in Fig. 6.3. This methodology is easily extended to account for a three dimensional decomposition. Fig. 6.4 shows a possible sequence of entry node connected in a three dimensional space. The branches of $\mathcal{T}$ will be included as constraints in the final MIQP, as explained in the following section. From this point

forward, references to the connectivity tree or $\mathcal{T}$ will regard the pruned tree.

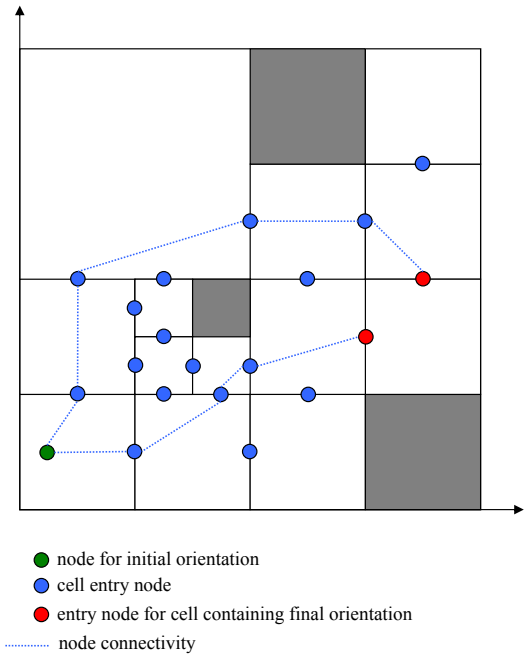

FIGURE 6.2: Example - Optimal Entry Node Connectivity, $\mathcal{G}^{\eta}_{opt}$

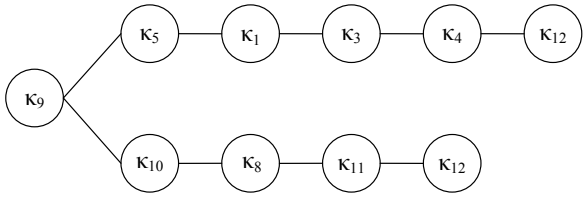

FIGURE 6.3: Example - Pruned Connectivity Tree, $\mathcal{T}$

6.2 Mixed Integer Representation of the Connectivity Tree

If the configuration of the robot at time step k is contained by any cell, $\kappa^i = [x^i_{min},\ x^i_{max}] \times [y^i_{min},\ y^i_{max}] \times [\theta^i_{min},\ \theta^i_{max}]$, i.e. $\kappa^i \ni \mathbf{x}_k$, the robot will not collide

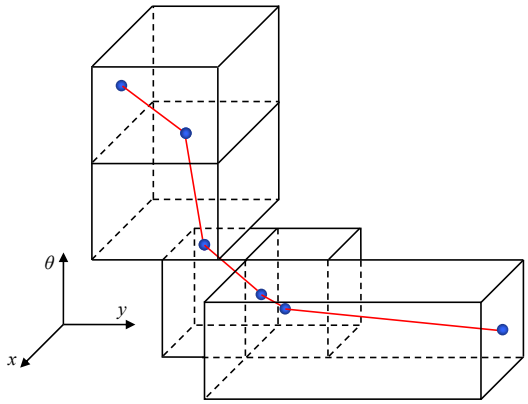

FIGURE 6.4: Example - Node Connectivity in Three Dimensions

with the obstacles. This condition is analogous to the following set of constraints

$$\begin{aligned} x^i_{min} \leq x_k \leq x^i_{max} \\ y^i_{min} \leq y_k \leq y^i_{max} \\ \theta^i_{min} \leq \theta_k \leq \theta^i_{max} \end{aligned} \tag{6.1}$$

Consider a branch, b_ℓ, in $\mathcal{T}$, where $\ell \in [1, \ldots, s]$ and s is the total number of branches. By definition, b_ℓ corresponds to an ordering of cells from κ^{init} to κ^{final}. Let $\Lambda[b_\ell]$ denote the length in cells of branch b_ℓ. If the robot is capable of following a kinematically feasible path in b_ℓ, it will avoid collisions with all obstacles along its trajectory. All cells in b_ℓ, $\kappa^i = b_\ell[i]\ \forall i \in [1, \ldots, \Lambda(b_\ell)]$, do not need to be considered as probable locations of the vehicle for all time steps k. In order to decrease the number of constraints at each time step, time allocations must be defined for each cell.

By inspection, the most time consuming path (without backtracking) through a cell κ^i is associated with entering through one corner, i.e. $(x^i_{min},\ y^i_{min})$, with orientation angle θ^i_{min} and exiting the cell at the diagonally opposite corner, i.e. (x^i_{max}, y^i_{max}), with orientation angle θ^i_{max}. The goal is to determine the number of discrete time steps required to traverse κ^i. This research proposed that the maximum number of time steps, Δk, necessary to enter and exit κ^i can be found by calculating the time requirement of an arc, α, across the cell, see Fig. 6.5. Consider a cell from

the quadtree ACD that has a square projection on the $x-y$ plane, i.e. $(x^i_{max}-x^i_{min}) = (y^i_{max}-y^i_{min})$. Let $\Delta x^i = (x^i_{max}-x^i_{min})$, $\Delta y^i = (y^i_{max}-y^i_{min})$ and $\Delta\theta^i = (\theta^i_{max}-\theta^i_{min})$; the length of the arc can be approximated as

$$\alpha = \frac{d}{2}\frac{\Delta\theta^i}{\sin\left(\Delta\theta^i/2\right)} \tag{6.2}$$

Where, by simple cell geometry,

$$d = \sqrt{2}\Delta x^i \tag{6.3}$$

The continuous time, t_α, to traverse the arc α is as follows

$$t_\alpha = \frac{\alpha}{v_{avg}} \tag{6.4}$$

where v_{avg} is an approximation of the velocity of the vehicle. In this research, v_{avg} was set to 75 % of the maximum allowable velocity, v_{max}. Using the above equations, Δk can be determined by

$$\begin{aligned}\Delta k &= \left\lceil \frac{t_\alpha}{\Delta t} \right\rceil \\ &= \left\lceil \left(\frac{\sqrt{2}\Delta x^i \Delta\theta^i}{v_{avg}\Delta t} \right) \frac{1}{\sin(\Delta\theta^i/2)} \right\rceil \end{aligned} \tag{6.5}$$

The value of Δk can be easily calculated for the varying cell dimensions of $\mathcal{K}_{void}$. The number of discrete time steps for a particular cell κ^i will be denoted as $\Delta k[\kappa^i]$.

Once again consider a branch, b_ℓ, of the connectivity tree $\mathcal{T}$. By applying the Δk-rule defined in Eqn. 6.5, the constraints requiring that a vehicle remain in the channel defined by b_ℓ can be approximated as

$k_{count} = 0$

for $i = 1 : \Lambda(b_\ell)$ **do**

$\kappa^i = b_\ell[i]$

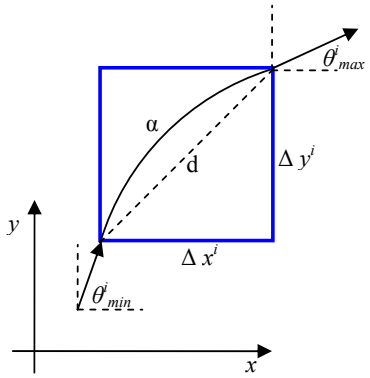

FIGURE 6.5: Determining Δk for a cell, κ^i

for $k = k_{count} : (k_{count} + \Delta k[\kappa^i])$ **do**

$x^i_{min} \leq x_k \leq x^i_{max}$

$y^i_{min} \leq y_k \leq y^i_{max}$

$\theta^i_{min} \leq \theta_k \leq \theta^i_{max}$

end for

$k_{count} = k_{count} + \Delta k[\kappa^i] + 1$

end for

A robot is only able to travel along a single channel between κ^{init} and κ^{final}. Consequently, only the constraints of one branch can be true along the optimal path. This condition can be addressed by introducing binary decision variables, β_ℓ, for each branch, b_ℓ, as follows

for $\ell = 1 : s$ **do**

$k_{count} = 0$

for $i = 1 : \Lambda(b_\ell)$ **do**

$\kappa^i = b_\ell(i)$

for $k = k_{count} : (k_{count} + \Delta k[\kappa^i])$ **do**

$x_k \leq x^i_{max} + M(1 - \beta_\ell)$

$x_k \geq x^i_{min} - M(1 - \beta_\ell)$

$$y_k \leq y^i_{max} + M(1 - \beta_\ell)$$

$$y_k \geq y^i_{min} - M(1 - \beta_\ell)$$

$$\theta_k \leq \theta^i_{max} + M(1 - \beta_\ell)$$

$$\theta_k \geq \theta^i_{min} - M(1 - \beta_\ell)$$

end for

$k_{count} = k_{count} + \Delta k[\kappa^i] + 1$

end for

end for

$$\sum_{\ell=1}^{s} \beta_\ell = 1$$

In the equations above big M theory has been used to address disjunctions between the branches. The final constraint in the statements above guarantees that only one branch of the tree is applied in the final trajectory calculation.

7

MIQP for Collision-Free Path Planning

Chapter 4 describes the procedure developed by this thesis to discretize the continuous, nonholonomic unicycle kinematics of the robot into a set of linear mixed integer constraints. These conditions, as well those defined for the free configuration space in Chapter 6, are included in the final optimization algorithm below. In order to provide a more realistic vehicle model, constraints on the maximum and minimum linear and angular velocities are introduced. These conditions are defined in the following section.

7.1 Velocity Constraints and Initial and Final Conditions

Additional constraints to those defined in Chapter 4 and Chapter 6 are required in the final mixed integer quadratic program (MIQP) to completely and realistically model a wheeled vehicle. In most motion planning scenarios the linear and angular velocities are each bounded by some maximum value as result of the physical limitations of the vehicle. For the discrete linear and angular velocities, with maximums v_{max} and

ω_{max}, respectively, the constraints are as follows

$$|v_k| \leq v_{max} \tag{7.1}$$

$$|\omega_k| \leq \omega_{max} \tag{7.2}$$

The above equations can be expressed by the linear constraints below

$$-v_{max} \leq v_k \leq v_{max} \tag{7.3}$$

$$-\omega_{max} \leq \omega_k \leq \omega_{max} \tag{7.4}$$

As stated in Chapter 2, the vehicle must begin in a prescribed initial configuration, $\mathbf{x}_{init}$. This condition is given by, where $\mathbf{x}(t = 0) = \mathbf{x}_0$

$$\mathbf{x}_0 = \mathbf{x}_{init} \tag{7.5}$$

Similarly, for the final (or goal) configuration, where $\mathbf{x}(t = T) = \mathbf{x}_N$

$$\mathbf{x}_N = \mathbf{x}_{final} \tag{7.6}$$

If the robot arrives at $\mathbf{x}_{final}$ before step N, i.e. $\mathbf{x}_k = \mathbf{x}_{final}$ for $k < N$, no additional cost is acquired based on the formulation of the optimization function, Eqn. 2.12.

7.2 Methodology Summary

Given a workspace $\mathcal{W}$, populated by n stationary, polygonal obstacles, a robot $\mathcal{A}$ with unicycle kinematics, and initial and goal configurations $\mathbf{x}_{init}$ and $\mathbf{x}_{final}$, the trajectory planning optimization is as follows. Begin by obtaining an approximate cell decomposition of the configuration space, $\mathcal{K}_{void}$, via the quadtree approach. Then, using the adjacency relationships of the cells, construct a connectivity graph, $\mathcal{G}$, of the workspace. This graph is then used to determine the connectivity of the entry nodes of the cells, $\mathcal{G}^\eta$. Using Dijkstra's algorithm prune $\mathcal{G}^\eta$ for optimal sequences of nodes between the initial node and the entry nodes of the final cell. These sequences

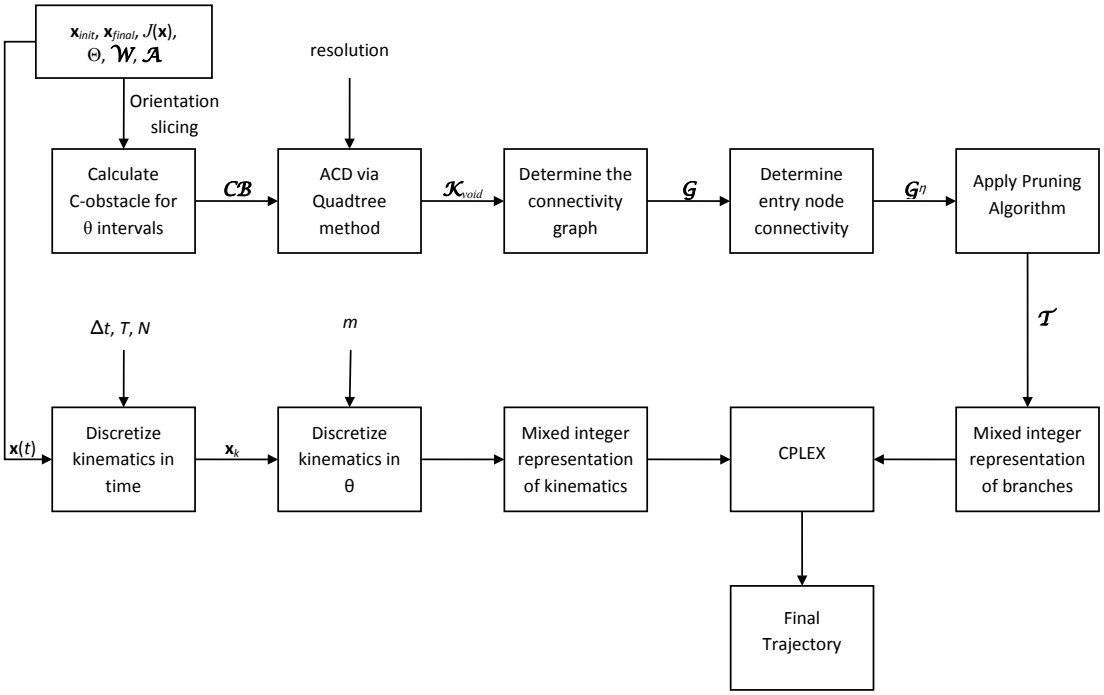

FIGURE 7.1: Summary of Methodology

will be mapped back to their corresponding cells, resulting in a pruned connectivity tree, $\mathcal{T}$.

At this point, the optimization over the L_2 norm of the state variables can be solved using MATLAB [50], and the Tomlab/CPLEX [51, 32] interface for MIQP. The final MIQP includes the discretized unicycle model (Chapter 4), the branch containment conditions (Chapter 6) and the set of additional constraints defined above. The complete optimization problem is defined below and summarized in Fig. 7.1.

$$\min_{\mathbf{x}} \; J(\mathbf{x}) = \sum_{k=1}^{N} (\mathbf{x}_k - \mathbf{x}_{k-1})^{\mathrm{T}} (\mathbf{x}_k - \mathbf{x}_{k-1})$$

Subject to:

$\mathbf{x}_0 = \mathbf{x}^{init} \quad \mathbf{x}_N = \mathbf{x}^{final}$

for $k = 0 : N - 1$ **do**

$-v_{max} \leq v_k \leq v_{max}$

$-\omega_{max} \leq \omega_k \leq \omega_{max}$

for $j = 1 : m$ **do**

$$A^j = \begin{bmatrix} 1 & 0 & 0 \\ 0 & 1 & 0 \\ 0 & 0 & 1 \end{bmatrix}$$

$$B^j = \begin{bmatrix} \Delta t \ \cos\phi^j_{mid} & 0 \\ \Delta t \ \sin\phi^j_{mid} & 0 \\ 0 & \Delta t \end{bmatrix}$$

$\mathbf{x}_{k+1} \leq A^j\mathbf{x}_k + B^j\mathbf{u}_k + M(1-\delta^j_k)$

$\mathbf{x}_{k+1} \geq A^j\mathbf{x}_k + B^j\mathbf{u}_k - M(1-\delta^j_k)$

$\theta_k \leq \phi^j + M(1-\delta^j_k)$

$\theta_k \geq \phi^{j-1} - M(1-\delta^j_k)$

$\delta^j_k = 0$ or 1

end for

$$\sum_{j=1}^{m} \delta^j_k = 1$$

end for

for $\ell = 1 : s$ **do**

$k_{count} = 0$

for $i = 1 : \Lambda(b_\ell)$ **do**

$\kappa^i = b_\ell(i)$

for $k = k_{count} : (k_{count} + \Delta k[\kappa^i])$ **do**

$x_k \leq x^i_{max} + M(1-\beta_\ell)$

$x_k \geq x^i_{min} - M(1-\beta_\ell)$

$y_k \leq y^i_{max} + M(1-\beta_\ell)$

$y_k \geq y^i_{min} - M(1-\beta_\ell)$

$\theta_k \leq \theta^i_{max} + M(1-\beta_\ell)$

$$\theta_k \geq \theta^i_{min} - M(1 - \beta_\ell)$$

end for

$k_{count} = k_{count} + \Delta k[\kappa^i] + 1$

end for

$\beta_\ell = 0$ or 1

end for

$$\sum_{\ell=1}^{s} \beta_\ell = 1$$

The following chapter documents the results obtained for various workspaces using the methodology defined above.

8

Results

This chapter presents a handful of trajectory simulations obtained via the methodology developed in this thesis. The algorithm was implemented in CPLEX, [32], a commercially available optimization software, using a Tomlab, [51], interface for MATLAB, [50]. The following values were used in the path simulations of a 1 unit by 2 unit rectangular robot: $\Delta t = 0.75$ s, $v_{max} = 5$ units/s, $\omega_{max} = 0.20$ rad/s, $\Delta\theta = \pi/6$ rad (θ discretization of all cells), and $m = 21$ (discretization of the kinematics). From here on, $\mathcal{A}$ will indicate the initial configuration of the vehicle in the pictorial results.

8.1 Kinematic Trajectory Planning

Before addressing obstacle avoidance concerns, the kinematic constraints developed by this research, see Chapter 4, were tested. Fig. 8.1 shows the optimization of the discretized cost function for a robot with initial configuration $\mathbf{x}_{init} = [4, 4, 0]^{\mathrm{T}}$ and final configuration $\mathbf{x}_{final} = [4, 6, \pi]^{\mathrm{T}}$. The trajectory returned for this scenario shows that the PWLTI representation of the vehicle maneuverability is an effective and useful discretization of the unicycle kinematics. An important consideration to take

into account when analyzing the paths of unicycle-like robots is that $v(t) = 0$, and consequently, $v_k = 0$, are admissible control inputs for the continuous and discrete linear velocities, respectively. Physically, this means that the robot is capable of rotating in Θ while remaining stationary in $\mathcal{W}$, i.e. rotating in place. As this is generally not the case for real vehicles, many models impose constraints on the turning radius or steering angle of the robot, [38]. However, as this is an initial stage of research, this thesis allowed the robot to rotate without translation, as is typical of the unicycle model. Fig. 8.2 documents a similar path, but over a longer distance where $\mathbf{x}_{final} = [4, 10, \pi]^{\mathrm{T}}$.

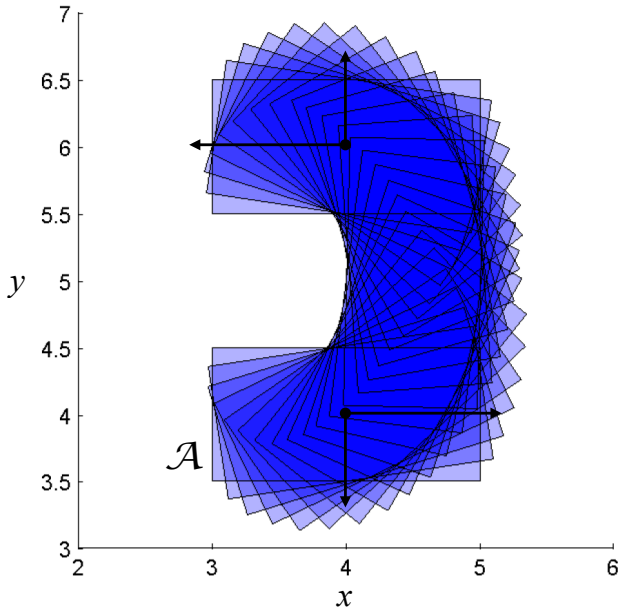

FIGURE 8.1: Kinematics - Path A

The numerical simulations shown in Fig. 8.3 and Fig. 8.4 depict the importance of the orientation angle of the vehicle in Θ. In both scenarios, the vehicle begins in state $\mathbf{x}_{init} = [4, 4, 0]^{\mathrm{T}}$ and ends with the centroid of the platform at $(x, y) = (12, 6)$. In Fig. 8.3 the robot begins and ends with orientation angle at 0 rad, resulting in a relatively simple trajectory between the initial and final states. Fig. 8.4, on the

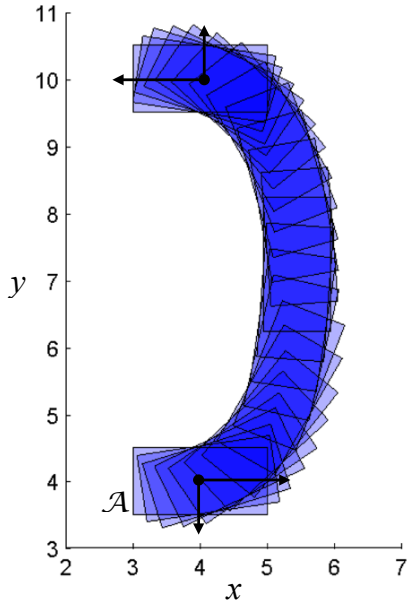

FIGURE 8.2: Kinematics - Path B

other hand, exhibits a more complicated path. In this case the vehicle begins at 0 rad and ends facing the opposite direction at π rad. The importance of this simulation is that given certain conditions traveling in reverse results may result in the optimal path, as is the case in many real world problems.

The results found in Fig. 8.1 - 8.4 show various paths obtained via the PWLTI representation of the vehicle kinematics. These simulations exhibit that the methodology developed can effectively discretize the nonholonomic relationships of the unicycle model and retain the original maneuverability.

8.2 Workspace 1

Following the verification of the vehicle kinematics, the connectivity tree methodology was tested as a means of obstacle avoidance for a simple workspace. The workspace was decomposed using the quadtree technique with a minimum resolution of 0.5 units. Fig. 8.5 demonstrates the maneuverability of a robot in a two

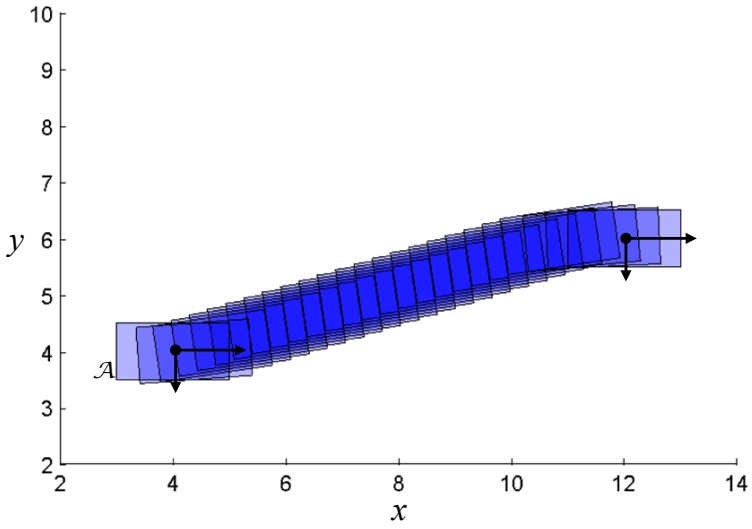

FIGURE 8.3: Kinematics - Path C

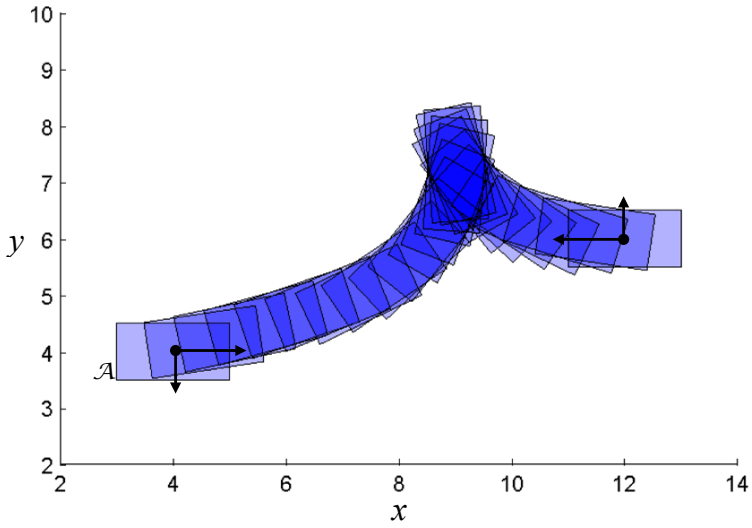

FIGURE 8.4: Kinematics - Path D

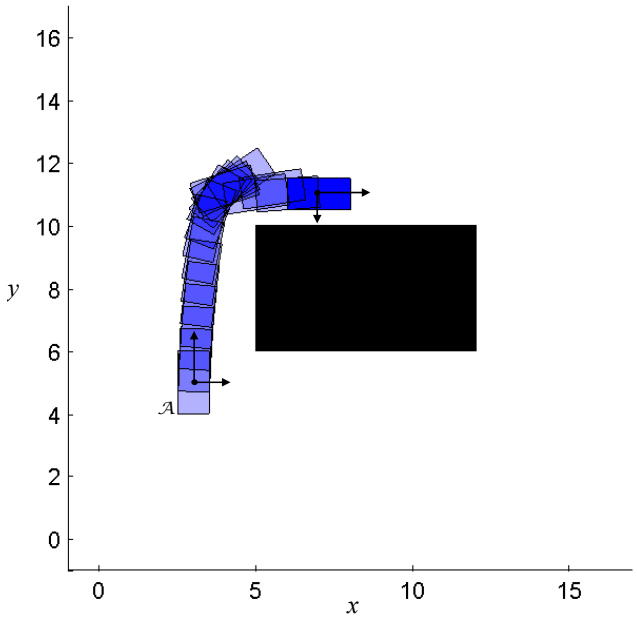

FIGURE 8.5: Workspace 1

dimensional workspace containing a single convex obstacle. The path arrived at in this workspaces exhibits the ability of the methodology developed in this thesis to address obstacle avoidance simultaneously with kinematic considerations.

8.3 The Parking Garage Problem

The following simulations require a robot to "park" in different workspace "garages" which are modeled as concave obstacles. The results obtained show that the robot is able to traverse small channels in concave environments, a limitation of other techniques. This is a marked improvement on previous disjunctive programming (DP) methodologies, which were unable to address concave workspaces, as shown in Chapter 3.3. Both Fig. 8.6 and Fig. 8.7 show simulations for two different, successful parking maneuvers in the workspace.

The environment found in Fig. 8.8, and the initial and final configurations of

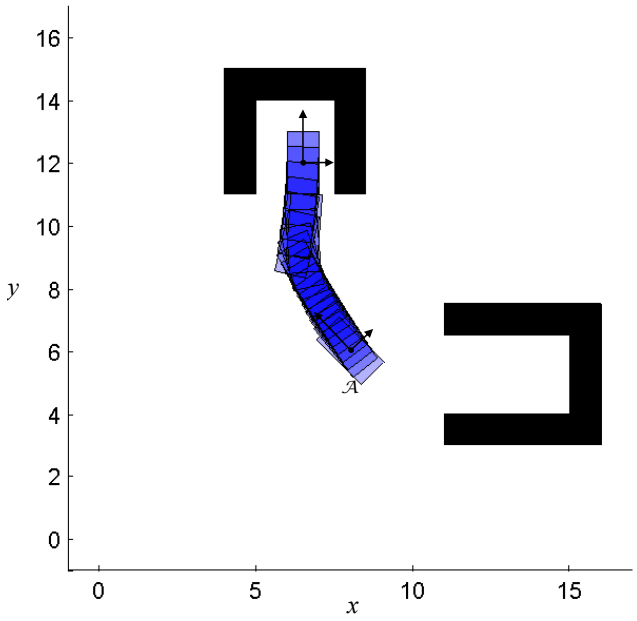

FIGURE 8.6: Parking Garage - Path A

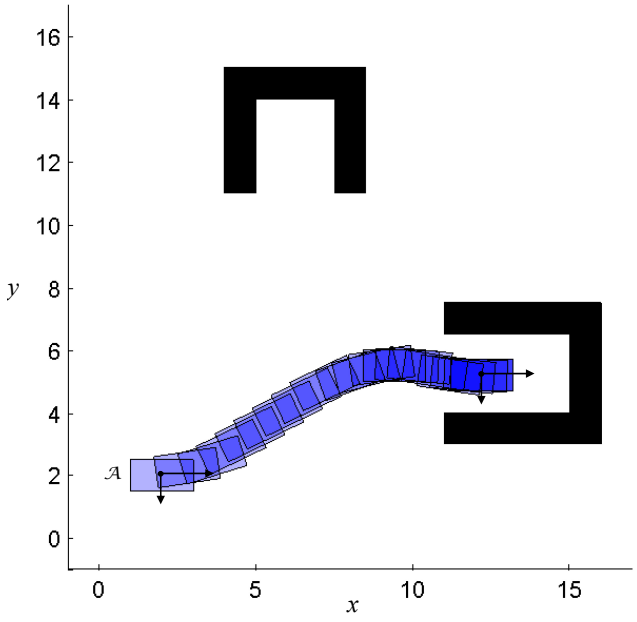

FIGURE 8.7: Parking Garage - Path B

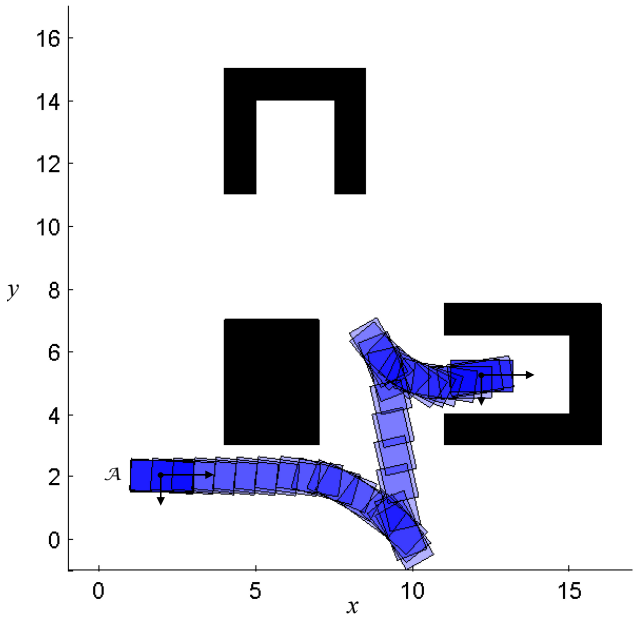

FIGURE 8.8: Parking Garage - Path C

the robot, are identical to those used in the simulation in Fig. 8.7, but with an added convex obstacle. The presence of the additional obstacle results in a dramatically different trajectory. This simulation shows that the methodology developed is able to address more complicated workspaces, and return relatively complicated kinematically feasible paths.

8.4 Workspace 2

The trajectory results in Fig. 8.9 and Fig. 8.10 exhibit that the technique established in this research is applicable to larger workspaces. These results show that the methodology can be used in a wide range of environments. By considering a causal relationship between the decomposed cells, the connectivity tree technique is able to effectively and efficiently address large workspaces.

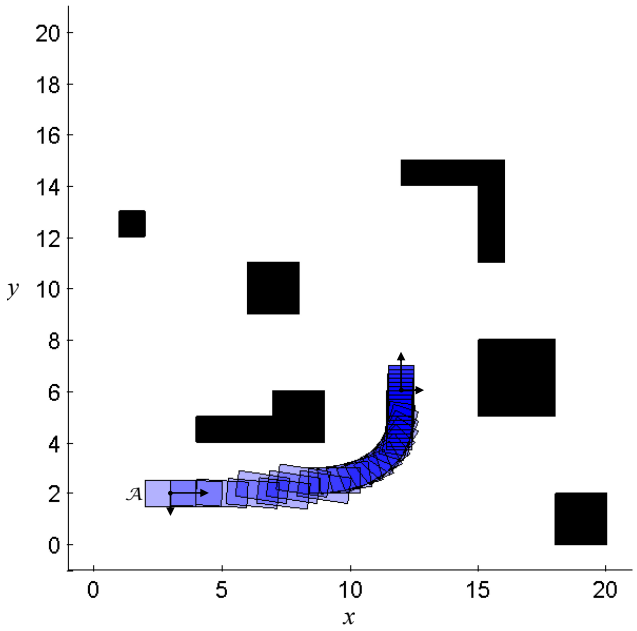

FIGURE 8.9: Workspace 2 - Path A

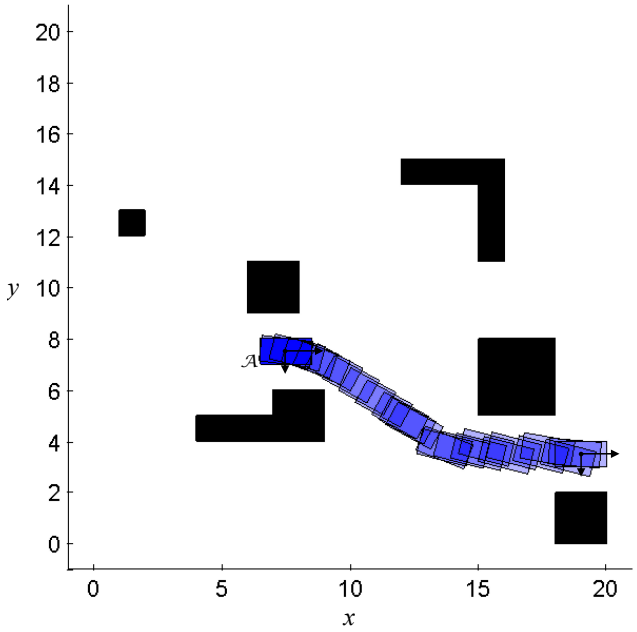

FIGURE 8.10: Workspace 2 - Path B

9

Conclusions

Due to the growing need for autonomous systems in both military and civilian applications, a large amount of research effort has been focused on the class of robotic motion planning problems. This class of problems has been used in a variety of applications ranging from mine-detection to mobile router connectivity, [18]. The research discussed in this thesis concentrated on one of the fundamental paradigms of trajectory planning, the *find-path* problem. In this benchmark problem, the robot must navigate an obstacle populated environment while avoiding collisions with stationary obstacles, the positions and geometries of which are assumed known *a priori*. This paradigm is well researched in the robotics community, and, as a result, a plethora of solution methods has been developed. The focus of this research was on the cell decomposition and the mathematical programming classes of motion planners. Both of these methods have been shown to be *complete*, or, at least, *resolution complete* planning algorithms, and are also considered to be *global* methodologies, [6].

Cell decomposition methodologies are able to effectively address obstacle avoidance concerns, [14], however many of these techniques are not readily extended to solve for optimal control problems in a manner that would be able to guarantee opti-

mality. Cell decomposition of workspaces are both time and memory demanding, as the volume of the decomposition grows exponentially with the degrees of freedom of the vehicle. Mixed integer programming (MIP) is a mathematical programming techniques that has been successfully implemented for optimal control problems. These methods are complete and are accomplished directly in the workspace, rather than a higher dimensional space, such as the configuration space. An added benefit is that MIP techniques are readily applied to convex obstacle avoidance, without any preprocessing of the workspace. MIP methods are revered for their flexibility and ability to address a variety of optimal control problems, while guaranteeing optimality. However, these techniques suffer from a handful of restrictions. For one, they are not readily applicable to concave obstacles or rotating vehicles. Furthermore, the computation requirements of solving MIP grow drastically with the number of binary variables.

This these proposes a combination of MIP and cell decomposition. Results show that the method is able to address many of the concerns of both MIP and cell decomposition techniques. In particular, the methodology is able to handle concave obstacles, rotating vehicles, and the optimal control problem. Furthermore, this research presents a novel discretization of the nonholonomic unicycle model in the form of a piece-wise linear time invariant system, resulting in a set of mixed integer constraints that can be easily included in a final optimization problem.

9.1 Summary of Results

The simulations depicted in Chapter 8 show the effectiveness of the methodology in addressing obstacle avoidance in a variety of different workspaces while simultaneously considering kinematic constraints. This thesis extends previous work in mixed integer programming for motion planning, which modeled vehicles as free-flying robots without geometries, to scenarios including vehicle geometries, rotation,

and kinematic considerations. The PWLTI approach proves to be an efficient and easily implemented approximation of the nonholonomic unicycle model.

By use of the entry node pruning algorithm defined in Chapter 6, the methodology was able to retain multiple channels in which a kinematically feasible path could exist. Although results can be obtained using the pruning algorithm defined, further research is needed to better address the dichotomy of optimal control and geometric planning problems. This methodology assigned weights to the connectivity tree using purely geometric considerations. Future research will examine alternative methods for pruning including alternative weighting metrics and different definitions of nodes in the workspace. In addition, this work will investigate kinematic considerations in tree branches, similar to the work found in [28, 29, 52]. Furthermore, the pruning algorithm in its current form is not able to claim completeness or optimality. Proofs regarding these important characteristics, as well as a complexity analysis, must be accomplished in order to determine the viability of the technique developed in this thesis.

9.2 Future Work

This research considered the simple trajectory planning problem of a single robot in an obstacle populated environment. Using the same paradigm, alternative kinematic and dynamic constraints can be explored using the mixed-integer framework. Aside from maneuverability considerations, a variety of other problems can be considered. These include stationary and dynamic target detecting [15, 53], sensor planning and control [54], and iterative applications of MIPs. Although a number of possible directions exist for future research, the first step will be in determining a pruning algorithm that takes into account kinematic considerations, and which can guarantee solution optimality.

Bibliography

[1] Y. K. Hwang and N. Ahuja, "Gross motion planning: a survey," *ACM Comput. Surv.*, vol. 24, no. 3, pp. 219–291, Sep. 1992.

[2] M. H. Overmars and P. Svestka, "A probabilistic learning approach to motion planning," Utrecht University, Netherlands, Scientific Report, jan 1994.

[3] J. Barraquand and J.-C. Latombe, "Robot motion planning: a distributed representation approach," *Int. J. Rob. Res.*, vol. 10, no. 6, pp. 628–649, Dec. 1991.

[4] J. Barraquand, B. Langlois, and J.-C. Latombe, "Numerical potential field techniques for robot path planning," *Systems, Man and Cybernetics, IEEE Transactions on*, vol. 22, no. 2, pp. 224 –241, 1992.

[5] J. Barraquand and J.-C. Latombe, "On nonholonomic mobile robots and optimal maneuvering," in *Intelligent Control, 1989. Proceedings., IEEE International Symposium on*, sep 1989, pp. 340 –347.

[6] J. C. Latombe, *Robot Motion Planning*. Kluwer Academic Publishers, 1991.

[7] Y. Koren and J. Borenstein, "Potential field methods and their inherent limitations for mobile robot navigation," in *Robotics and Automation, 1991. Proceedings., 1991 IEEE International Conference on*, vol. 2, Apr 1991, pp. 1398 –1404.

[8] B. Donald, P. Xavier, J. Canny, and J. Reif, "Kinodynamic motion planning," *Association of Computing Machinery*, vol. 40, no. 5, pp. 1048–1066, 1993.

[9] J. van den Berg and M. Overmars, "Kinodynamic motion planning on roadmaps in dynamic environments," in *Intelligent Robots and Systems, 2007. IROS 2007. IEEE/RSJ International Conference on*, 2007, pp. 4253 –4258.

[10] S. M. LaValle, M. S. Branicky, and S. R. Lindermann, "On the relationship between classical grid search and probabilistic roadmaps," *International Journal of Robotics Research*, 2004.

[11] S. M. LaValle and J. J. K. Jr., "Randomized kinodynamic planning," *International Journal of Robotics Research*, vol. 20, no. 5, pp. 378–400, 2001.

[12] D. Hsu, R. Kindel, J.-C. Latombe, and S. Rock, "Randomized kinodynamic motion planning with moving obstacles," 2000.

[13] S. Ferrari and C. Cai, "Information-driven search strategies in the board game of clue," *Systems, Man, and Cybernetics, Part B: Cybernetics, IEEE Transactions on*, vol. 39, no. 3, pp. 607 –625, June 2009.

[14] C. Cai and S. Ferrari, "Information-driven sensor path planning by approximate cell decomposition," *Trans. Sys. Man Cyber. Part B*, vol. 39, no. 3, pp. 672–689, 2009.

[15] S. Ferrari, R. Fierro, B. Perteet, C. Cai, and K. Baumgartner, "A geometric optimization approach to detecting and intercepting dynamic targets using a mobile sensor network," *SIAM J. Control Optim.*, vol. 48, no. 1, pp. 292–320, 2009.

[16] L. Blackmore and B. Williams, "Optimal manipulator path planning with obstacles using disjunctive programming," in *American Control Conference*, 2006.

[17] T. Schouwenaars, B. D. Moor, J. How, and E. Feron, "Mixed integer programming for multi-vehicle path planning," in *Proceedings of the European Control Conference*, 2001, pp. 2603–2608.

[18] N. Bezzo, R. Fierro, A. Swingler, and S. Ferrari, "A disjunctive programming approach for motion planning of mobile router networks," *International Journal of Robotics and Automation*, vol. 3, pp. 227–252, 2010.

[19] N. K. Yilmaz, C. Evangelinos, P. F. J. Lermusiaux, and N. M. Patrikalakis, "Path planning of autonomous underwater vehicles for adaptive sampling using mixed integer linear programming," *IEEE Journal of Oceanic Engineering*, vol. 33, no. 4, pp. 522–537, 2008.

[20] A. Richards, J. How, T. Schouwenaars, , and E. Feron, "Plume avoidance maneuver planning using mixed integer linear programming," in *Proceedings of AIAA Guidance Navigation and Control Conference*, 2001.

[21] A. Richards, T. Schouwenaars, J. How, and E. Feron, "Spacecraft trajectory planning with avoidance constraints using mixed-integer linear programming," *Journal of Guidance, Control, and Dynamics*, vol. 25, no. 4, pp. 755–764, 2002.

[22] L. Pallottino, E. Feron, and A. Bicchi, "Conflict resolution problems for air traffic management systems solved with mixed integer programming," vol. 3, no. 1, 2002.

[23] R. Fierro and K. Wesselowski, "Optimization-based control of multi-vehicle systems," in *Cooperative Control*, ser. Lecture Notes in Control and Information Sciences, V. Kumar, N. Leonard, and A. Morse, Eds., 2005, vol. 309, pp. 461–463.

[24] A. Richards, Y. Kuwata, and J. How, "Experimental demonstrations of real-time milp control," in *In Proceeding of the AIAA Guidance, Navigation, and Control Conference*, 2003.

[25] H. Ding, M. Zhou, and O. Stursberg, "Optimal path planning in the workspace for articulated robots using mixed integer programming," in *Intelligent Robots and Systems, 2009. IROS 2009. IEEE/RSJ International Conference on*, oct. 2009, pp. 5770 –5775.

[26] T. Schouwenaars, J. How, and E. Feron, "Receding horizon path planning with implicit safety guarantees," in *Proceedings of the American Control Conference*, 2004, pp. 5576–5581.

[27] M. G. Earl and R. D'Andrea, "Iterative milp methods for vehicle-control problems," *IEEE Transactions on Robotics*, vol. 21, no. 6, pp. 1158 –1167, 2005.

[28] R. Cowlagi and P. Tsiotras, "On the existence and synthesis of curvature-bounded paths inside nonuniform rectangular channels," in *American Control Conference (ACC), 2010*, 2010, pp. 5382 –5387.

[29] ——, "Kinematic feasibility guarantees in geometric path planning using history-based transition costs over cell decompositions," in *American Control Conference (ACC), 2010*, 2010.

[30] R. A. Brooks and T. Lozano-Perez, "A subdivision algorithm in configuration space for findpath with rotation," in *Proceedings of the Eighth International Joint Conference on Artificial Intelligence*, 1983, pp. 799–806.

[31] D. E. Kirk, *Optimal Control Theory: An Introduction*. Prentice-Hall Inc., 1970.

[32] *ILOG CPLEX 9.0 User's Manual*, ILOG, 2003.

[33] A. Bemporad and M. Morari, "Control of systems integrating logic, dynamics, and constraints," *Automatica*, vol. 35, pp. 407–427, 1998.

[34] A. Bemporad, G. Ferrari-Trecate, and M. Morari, "Observability and controllability of piecewise affine and hybrid systems," *IEEE Transactions on Automatic Control*, vol. 45, pp. 1864–1876, 2000.

[35] A. Richards and J. P. How, "Aircraft trajectory planning with collision avoidance using mixed integer linear programming," in *Proceedings of the American Controls Conference*, 2002, pp. 1936–1941.

[36] P. Morin and C. Samson, *Motion Control of Wheeled Mobile Robots*, 2008, pp. 779–826.

[37] A. D. Luca, G. Oriolo, and C. Samson, *Robot Motion Planning and Control: Lectures Notes in Control and Information Sciences 229*. Springer, ch. Feedback Control of a Nonholonomic Car-Like Robot, pp. 170–253.

[38] D. Anisi, "Optimal motion control of a ground vehicle," Swedish Defense Research Agency, Stockholm, Sweden, Scientific Report, July 2003.

[39] J. Barraquand and J. C. Latombe, "Controllability of mobile robots with kinematic constraints," Stanford University, Stanford, CA, Research, June 1990.

[40] K. Kedem and M. Sharir, "An efficient algorithm for planning collision-free translational motion of a convex polygonal object in 2-dimensional space amidst polygonal obstacles," in *Proceedings of the First Annual Symposium on Computational geometry*, ser. SCG '85. New York: ACM, 1985, pp. 75–80.

[41] F. Avnaim, J. Boissonnat, and B. Faverjon, "A practical exact motion planning algorithm for polygonal objects amidst polygonal obstacles," in *Proceedings of the International Conference on Robotics and Automation*, vol. 3, April 1988, pp. 1656 –1663.

[42] J. Schwartz and M. Sharir, "On the 'piano movers' problem: Ii. general techniques for computing topological properties of real algebraic manifolds," *Advances in Applied Mathematics*, vol. 4, pp. 298–351, 1983.

[43] K. Kedem and M. Sharir, "An efficient motion planning algorithm for a convex polygonal object in 2-dimensional polygonal space," New York University, New York, Robotics Report 90, October 1986.

[44] N. I. Katevas, S. G. Tzafestas, and C. G. Pnevmatikatos, "The approximate cell decomposition with local node refinement global path planning method: Path nodes refinement and curve parametric interpolation," *J. Intell. Robotics Syst.*, vol. 22, no. 3-4, pp. 289–314, 1998.

[45] D. Zhu and J. C. Latombe, "New heuristic algorithm for efficient hierarchical path planning," *IEEE Transactions on Robotics and Automation*, vol. 7, no. 1, pp. 9–19, 1991.

[46] A. Swingler and S. Ferrari, "A cell decomposition approach to cooperative path planning and collision avoidance via disjunctive programming," in *Proc. of IEEE Conf. Decision and Control*, Atlanta, GA, 2010, pp. 6329–6336.

[47] H. Samet, "The quadtree and related hierarchical data structures," *ACM Comput. Surv.*, vol. 16, no. 2, pp. 187–260, Jun. 1984.

[48] S. M. LaValle, *Planning Algorithms*. Cambridge University Press, 2006.

[49] D. Gleich, "gaimc: Graph algorithms in matlab code," May 2009. [Online]. Available: https://github.com/dgleich/gaimc

[50] MathWorks, "Matlab r2011a." [Online]. Available: http://www.mathworks.com/products/matlab/

[51] K. Holmstrom, A. Goran, and M. Edvall, *User's Guide for Tomlab 7*, TOMLAB OPTIMIZATION, 2009. [Online]. Available: http://tomopt.com/docs/TOMLAB.pdf

[52] A. Scheuer and T. Fraichard, "Continuous-curvature path planning for car-like vehicles," in *Intelligent Robots and Systems, 1997. IROS '97., Proceedings of the 1997 IEEE/RSJ International Conference on*, vol. 2, Sep 1997, pp. 997 –1003.

[53] W. Lu, G. Zhang, and S. Ferrari, "A comparison of information theoretic functions for tracking maneuvering targets."

[54] G. Zhang, W. Lu, and S. Ferrari, "An information potential approach to integrated sensor planning and control."